NASA TECHNICAL MEMORANDUM

NASA TM X-1030

NASA TM X-1030

LONGITUDINAL AERODYNAMIC CHARACTERISTICS OF A MODEL OF A HORIZONTAL-TAKE-OFF REUSABLE LAUNCH VEHICLE AT MACH NUMBERS FROM 3 TO 6

by Larry R. Clark and John P. Decker

Langley Research Center

Langley Station, Hampton, Va.

NATIONAL AERONAUTICS AND SPACE ADMINISTRATION • WASHINGTON, D. C. • OCTOBER 1964

LONGITUDINAL AERODYNAMIC CHARACTERISTICS OF A MODEL OF A HORIZONTAL-TAKE-OFF REUSABLE LAUNCH VEHICLE AT MACH NUMBERS FROM 3 TO 6

By Larry R. Clark and John P. Decker

Langley Research Center
Langley Station, Hampton, Va.

NATIONAL AERONAUTICS AND SPACE ADMINISTRATION

LONGITUDINAL AERODYNAMIC CHARACTERISTICS OF A MODEL OF A HORIZONTAL-TAKE-OFF REUSABLE LAUNCH VEHICLE AT MACH NUMBERS FROM 3 TO 6*

By Larry R. Clark and John P. Decker
Langley Research Center

SUMMARY

A wind-tunnel investigation was made at supersonic and hypersonic speeds of an approximate 1/125-scale model of a conceptual multistage horizontal-take-off reusable launch vehicle. The model consisted of a winged reusable first stage with a canard, a winged reusable second stage, and a winged third-stage reusable spacecraft with an expendable maneuver propulsion package. The two upper stages were arranged in tandem, and this combination was placed parallel to the first-stage reusable booster in piggyback position. The model was tested at Mach numbers of 3, 4.5, and 6, at angles of attack from about -4° to 19°, and at an angle of sideslip of 0°. The test Reynolds numbers per foot varied from approximately 1.0×10^6 to 2.1×10^6.

For the selected moment reference center, the complete first stage was longitudinally stable at zero lift at a Mach number of 3, but was unstable at Mach numbers of 4.5 and 6. However, the canard produced sizable destabilizing increments, and the first stage without the canard was stable at Mach numbers of 3 and 4.5 with marginal stability at a Mach number of 6. Maximum lift-drag ratios for the complete first stage decreased from about 4.57 to 3.85 as the test Mach number was increased from 3 to 6. Including the fuselage base drag reduced the maximum lift-drag ratios of the complete first stage about 17 percent at a Mach number of 3 and about 6 percent at a Mach number of 4.5 and had a negligible effect at a Mach number of 6. The addition of the complete upper stages to the complete first stage caused destabilizing increments longitudinally and resulted in increases in drag at zero lift of almost 100 percent at all test Mach numbers.

INTRODUCTION

A research program is being conducted at the Langley Research Center to study some of the aerodynamic problems associated with horizontal-take-off and vertical-take-off winged reusable orbital launch vehicles. Results of

*Title, Unclassified.

investigations on models of reusable launch vehicles representing these concepts are given in references 1 to 6. The present tests are a continuation into the supersonic and hypersonic speed ranges of an investigation of a conceptual horizontal-take-off reusable launch vehicle for which low-speed results were reported on a larger scale model in reference 6. In general, the present vehicle is different from the horizontal-take-off vehicle in references 2, 3, and 5 in that it has a large volume fuselage and the second stage was winged and thus intended to be reusable.

The launch vehicle consisted of a winged reusable first stage with a canard, a winged reusable second stage, and a winged third-stage reusable spacecraft with an expendable propulsion package for in-orbit maneuvering. The upper stages were arranged in tandem, and this combination was placed parallel to the first stage in a piggyback fashion. The first-stage canard was incorporated primarily to satisfy the control requirements of the first stage during its reentry phase.

All stages of the vehicle were conceived to employ rocket engines using liquid oxygen and hydrogen propellants during boost. The first stage was assumed to utilize turbojet engines as its return propulsion system during subsonic flight, whereas the second and spacecraft stages were considered to be glide return vehicles.

The launch vehicle was designed to place a maximum of 20,000 pounds of spacecraft into a low earth orbit. The vehicle was conceived to be accelerated to a take-off velocity of 500 fps by some type of device such as a sled. The launch vehicle was assumed to be rocket powered and to perform a rapid pull-up, keeping the total acceleration between 2.5g and 3.0g, to get into a ballistic trajectory and minimize the gravity losses. Stage separation was estimated to occur at a speed of 6500 fps at an altitude of about 230,000 feet, and the take-off wing loading was assumed to be 120 lb/sq ft, based on total wing area.

Tests were conducted on a 1/125-scale model in the 2-foot hypersonic facility at the Langley Research Center at Mach numbers of 3, 4.5, and 6, at angles of attack from approximately -4° to 19°, and at an angle of sideslip of 0°. The Reynolds numbers per foot varied from approximately 1.0×10^{6} to 2.1×10^{6}.

SYMBOLS

The aerodynamic characteristics of the model are referred to the stability axes. The moment reference center was chosen to be 15 percent of the mean aerodynamic chord of the first-stage wing, and was 7.48 inches forward of the model base in the stage-separation plane as shown in figure 1. All aerodynamic coefficients are based on the geometry of the first-stage reusable booster.

C_L lift coefficient, $\frac{\text{Lift}}{qS}$

$C_{L,(L/D)_{max}}$ lift coefficient at maximum lift-drag ratio

C_D	drag coefficient, $\frac{\text{Drag}}{qS}$
C_m	pitching-moment coefficient, $\frac{\text{Pitching moment}}{qS\bar{c}}$
C_{L_α}	lift-curve slope at zero lift, $\frac{\partial C_L}{\partial \alpha}$, per deg
$C_{m_{C_L}}$	longitudinal-stability parameter at zero lift, $\frac{\partial C_m}{\partial C_L}$
C_{m_δ}	control-effectiveness parameter of canard at zero lift, $\frac{\partial C_m}{\partial \delta}$, per deg
$\frac{\partial C_D}{\partial {C_L}^2}$	drag-due-to-lift parameter
c	local chord, ft
$\bar{c}$	reference mean aerodynamic chord based on total wing area, 0.733 ft
L/D	lift-drag ratio, $\frac{C_L}{C_D}$
M	free-stream Mach number
p_t	stagnation pressure, atm
q	free-stream dynamic pressure, lb/sq ft
S	reference wing area, 0.440 sq ft
T_t	stagnation temperature, $^{\circ}R$
α	angle of attack, deg
δ	angle of canard deflection (positive for leading edge up), deg

Subscripts:

o	condition at zero lift
max	maximum

Component designations:

B	fuselage, first- or second-stage
W	wing, first- or second-stage
C^0	canard, $\delta = 0^\circ$
C^{-5}	canard, $\delta = -5^\circ$
C^5	canard, $\delta = 5^\circ$
N	nacelles, first-stage
F	vertical fins, first- or second-stage
M	maneuver propulsion package
S	spacecraft with mounting pad
S'	spacecraft without mounting pad (lowered 0.3 inch)

DESCRIPTION OF MODEL

The complete launch vehicle and its components are shown in figure 1. The launch vehicle consisted of a winged reusable first stage with a canard, a winged reusable second stage, and a winged third-stage reusable spacecraft with an expendable space-maneuvering propulsion package. The two upper stages were arranged in tandem, and this combination was placed parallel to the first-stage reusable booster in a piggyback position. Principal model dimensions are presented in table I, and photographs of the model are shown in figure 2.

First-stage reusable booster.- The first-stage reusable booster consisted of a semicylindrical fuselage with an ogival forebody, a delta canard, and a delta wing with trapezoidal vertical fins mounted outboard on nacelles. (See fig. 1(b).) The first-stage wing was flat on the upper surface rearward of the 40-percent-chord station to allow mating with the second-stage wing. The requirement for a flat upper surface resulted in a wing dihedral angle of about $3\frac{1}{2}^\circ$. A wedge or boattail on the lower surface of the wing extended from 0.85c to the wing trailing edge. (See fig. 1(c).) The exposed area of the canard was approximately 7 percent of the total first-stage wing area, and the distance between $0.25\bar{c}$ of the canard and $0.25\bar{c}$ of the first-stage wing was $1.4\bar{c}$ of the wing. Provision was made for testing the canard at 0° and $\pm 5^\circ$.

The first-stage vertical fins were located outboard at 2/3 of the wing semispan and the total fin area, which was equally distributed above and below the wing, was approximately 15 percent of the total wing area. The vertical fins had a panel aspect ratio of 1.15 and a taper ratio of 0.5. The nacelles were cylindrical with a parabolic nose and were considered to house the flyback engines. The nacelles formed the juncture between the first-stage wing and vertical fins.

Second-stage reusable booster.- The second-stage reusable booster consisted of a cylindrical fuselage $7\frac{1}{2}$ diameters long (including an interstage of 1 diameter length to allow for the nose of the second-stage fuselage) and a trapezoidal wing with two outboard-mounted vertical fins located at 2/3 of the wing semispan. The fuselage incorporated a side fairing which extended vertically from the center line of the second-stage fuselage to the upper surface of the first-stage fuselage.

The second-stage wing thickness was chosen to achieve a total profile thickness of 0.065c (based on the chord of the first-stage wing) when the first- and second-stage wings were mated. The upper surface of the second-stage wing was an extension of the upper wedge surface of the first-stage wing; that is, the two upper wedge surfaces were coplanar. A portion of the leading edge of this extension was removed to form a constant leading-edge radius on the second-stage wing identical to that of the first-stage wing. The purpose of this arrangement was to reduce the interference of the mated wings during launch. The second-stage vertical fins were almost identical to the first-stage vertical fins, but only the upper element was employed.

Orbital stage.- The orbital stage consisted of a spacecraft and a maneuver propulsion package. The spacecraft was a wing-body configuration with toed-in wing-tip-mounted vertical fins. (See fig. 1(d).) The spacecraft wing was unsymmetrical with the camber adjacent to the spacecraft pad, and the span (including vertical fins) was approximately equal to the width of the first-stage fuselage. The maneuver propulsion package was an expendable rocket booster which was 3 diameters long, including the spacecraft adapter fairing. It was a short cylinder with the same diameter as the second-stage fuselage and also incorporated the same type of side fairing as the second-stage fuselage. When the model was tested without the maneuver propulsion package, the spacecraft was moved rearward to connect directly with the second-stage fuselage. This configuration was considered to meet some other mission requirement not needing appreciable in-orbit maneuvering.

APPARATUS AND TESTS

The tests were conducted in the 2-foot hypersonic facility at the Langley Research Center (described in ref. 7) at nominal Mach numbers of 3, 4.5, and 6, at angles of attack from approximately -4° to 19°, and at an angle of sideslip of 0°. The test Reynolds numbers per foot varied from approximately 1.0×10^{6} to 2.1×10^{6}.

Static aerodynamic force and moment data were obtained by means of a six-component internally mounted strain-gage balance. All data were obtained with the model smooth, and at the Reynolds numbers of these tests laminar flow would be expected over the entire model. The angles of attack were corrected for balance and sting deflection under load. The drag of the vehicle was corrected to correspond to a base pressure equal to the free-stream static pressure on the first-stage reusable booster and that portion of the first-stage wing base intercepted by the fuselage. No pressure corrections were applied to the base area of the second-stage booster.

The average test conditions and Reynolds number variation during a typical launch trajectory for the complete vehicle and a typical flyback trajectory for the first stage are given in the following table:

M	p_t, atm	T_t, °R	Reynolds number (based on overall length of vehicle)		
			Test	Launch	Flyback
3.00	1.0	580	4.2×10^6	7.0×10^6	31×10^6
4.50	1.5	760	2.0×10^6	2.4×10^6	25×10^6
6.00	3.4	810	2.2×10^6	1.6×10^6	9×10^6

It is seen from this table that the Reynolds numbers for the launch trajectory are in close agreement to the test Reynolds numbers, but the Reynolds numbers for the flyback trajectory of the first stage are considerably higher.

The estimated accuracies of the coefficients based on instrument calibration are within the following limits:

C_D . . . . ±0.001
C_L . . . . ±0.003
C_m . . . . ±0.001

Model angles of attack are estimated to be accurate within ±0.2.

PRESENTATION OF RESULTS

The basic longitudinal aerodynamic characteristics are given in figures 3 to 6. Some results have been summarized in figures 7 to 10. An outline of the contents of the data figures is as follows:

In the data figures, the various components were indicated by letter symbols for purposes of configuration identification. (See symbol list for component designations.)

DISCUSSION

The basic longitudinal aerodynamic characteristics (figs. 3 to 6) have been summarized in figures 7 to 10. The discussion will indicate some stage and component effects on the longitudinal aerodynamic characteristics of the first-stage reusable booster and the take-off launch vehicle.

Lift Characteristics

First-stage reusable booster.- Figures 3(a) and 4(a) show that all the first-stage configurations generally exhibited small positive values of lift at zero angle of attack throughout the test Mach number range. These positive values at hypersonic speeds contrast with relatively large negative values at subsonic and transonic speeds shown in reference 6. At high angles of attack, the lift curves (figs. 3(a) and 4(a)) exhibit increasing nonlinearity with increasing Mach number, a result which is usually expected in this speed range.

The lift-curve slopes at zero lift for the complete first stage, shown in figure 7, decreased from about 0.023 to 0.016 as the test Mach number was increased from 3 to 6. The removal of the canard from the first stage caused some small reductions in C_{L_α} at Mach numbers of 4.5 and 6, but had a negligible effect on C_{L_α} at $M = 3$. The first-stage fuselage alone, presented in figure 3(a), is a high-lifting body which, at $M = 6$, is shown to carry as much lift at high angles of attack as the first-stage wing. The values of C_{L_α} for the complete first stage of the present tests agree reasonably well with values of C_{L_α} presented in reference 5 for a first-stage reusable booster employing a wedge-type delta wing. As was true for the vehicle in reference 5, values of C_{L_α} for the first stage of the present tests agree well with the supersonic flat-plate theory $\left(C_{L_\alpha} = \frac{4}{\sqrt{M^2 - 1}} \text{ per radian}\right)$. The largest disagreement with the theory occurred at Mach numbers of 4.5 and 6.0.

Launch vehicle.- The addition of the complete upper stages to the complete first stage resulted in decreases in lift coefficient at zero angle of attack of about 0.012 at each of the test Mach numbers. (Compare figs. 3(a) and 5(a).) Figures 5(a) and 6(a) indicate that further decreases in lift at zero angle of attack were obtained by removing the canard, the maneuver propulsion package, or the spacecraft pad (accompanied by lowering the spacecraft 0.3 inch).

In figure 7, it can be seen that the addition of the complete upper stages to the complete first stage reduced C_{L_α} approximately 8 to 10 percent at Mach numbers of 4.5 and 6, but had little effect on C_{L_α} at $M = 3$. In general, removal of the maneuver propulsion package and the spacecraft pad each resulted in some small increases in C_{L_α}, especially at $M = 6$. However, neither the canard nor the second- and first-stage vertical fins and nacelles had much effect on C_{L_α}.

Longitudinal Stability

First-stage reusable booster.- The complete first stage had positive values of $C_{m,o}$ between approximately 0.006 and 0.011 throughout the Mach number range of these tests (fig. 3(b)). Reference 6 showed that this same vehicle had positive values of $C_{m,o}$ between 0.03 and 0.05 at subsonic and transonic speeds. Neither the removal of the first-stage fins and nacelles nor the removal of the canard had a significant effect on $C_{m,o}$. Comparison of wing-on and wing-off data of figure 3(b) indicates that the first-stage wing was responsible for a sizable portion of the positive $C_{m,o}$ values of the first stage.

The complete first stage was longitudinally stable at zero lift about the selected moment reference center of $0.15\bar{c}$ at $M = 3$, but became increasingly unstable as the test Mach number was increased to 4.5 and 6 (fig. 8). Figure 3(b) reveals that even at $M = 3$ the vehicle became unstable at high lift coefficients. It can be observed in figure 8 that the aerodynamic center moved forward approximately $0.20\bar{c}$ as the test Mach number was increased from 3 to 6. However, removal of the canard produced sizable improvements in stability and resulted in a stable vehicle at $M = 3$ and 4.5 with about marginal stability at $M = 6$. The canard was also shown in reference 6 to be detrimental at subsonic and transonic speeds. The removal of the first-stage fins and nacelles resulted in some small destabilizing increments. The behavior of the fins and nacelles probably resulted from their end-plate effect which would prevent a large spanwise component of local flow and thereby effectively increase the wing loading at the rear of the vehicle. Figure 8 shows the fuselage alone to be a very unstable body.

The control-effectiveness parameter of the canard on the complete first stage at $C_L = 0$ decreased from about 0.0026 to 0.0019 as the test Mach number was increased from 3 to 6 (fig. 8). Increments in pitching moment resulting from canard deflection can be seen in figure 4(b) to remain nearly constant throughout the lift range. Values of C_{m_δ} at the Mach numbers of the present tests are generally less than those values shown in reference 6 for this vehicle at Mach numbers from 0.6 to 1.2. These differences in C_{m_δ} are caused primarily by the differences in the lift-curve slopes of the canard in the high and low speed ranges.

Launch vehicle.- The addition of the complete upper stages to the complete first stage caused small reductions in $C_{m,o}$ (compare figs. 3(b) and 5(b)). Figure 6(b) indicates that the canard had a negligible effect on $C_{m,o}$. However, figure 6(b) also reveals that the removal of the maneuver propulsion package, accompanied by moving the spacecraft rearward on the vehicle, caused increases in $C_{m,o}$ which became progressively larger with increases in Mach number and amounted to $C_{m,o} = 0.028$ at $M = 6$. The reason for these large $C_{m,o}$ increases resulting from moving the spacecraft rearward are thought to be twofold. First, the positive pressures caused by shocks off the front portion of the spacecraft were moved rearward and produced a shorter moment arm over which any negative lift created by these positive pressures would act. Secondly, the position of the spacecraft in this rearward position would probably result in some interference between the spacecraft and the first-stage wing. This interference is thought to be primarily in the nature of shock waves from the leading edge and nose portion of the spacecraft impinging on the upper surface of the wing and creating a positive pressure field which would result in reduced lift on the wing. Since the shocks would become more oblique with increases in Mach number, the pressure field would be further rearward at $M = 6$ and provide the largest positive pitching moment. Reference 5 also discusses the losses in lift on the first-stage wing of a reusable launch vehicle caused by moving a parallel-mounted winged spacecraft rearward on the vehicle.

Removal of the spacecraft pad with the accompanying downward shift of the spacecraft caused sizable increases in $C_{m,o}$ at all test Mach numbers (fig. 5(b)). This is thought to be the result of a reduction in the positive pressures at the front portion of the model generated by shocks off the spacecraft. With the pad removed, the shock system would probably be weaker, with a resultant loss in positive pressure forward of the vehicle moment reference center.

The addition of the complete upper stages to the complete first stage caused some decreases in longitudinal stability, especially at $M = 6$ (fig. 8). Removing the second- and first-stage fins and nacelles from the launch vehicle caused some small destabilizing increments, whereas removing the canard from the launch vehicle produced large stabilizing increments comparable to those obtained when the canard was removed from the first stage alone. Although the removal of the maneuver propulsion package, which resulted in moving the spacecraft rearward, caused large increases in $C_{m,o}$, the effect of its removal on $C_{m_{C_L}}$ was small.

Drag and L/D Characteristics

First-stage reusable booster.- Drag at zero lift for the complete first stage is shown in figure 9 which also indicates the drag contribution of the wing, canard, and the first-stage vertical fins and nacelles. Figure 9 shows that at $M = 6$, as an example, the fuselage alone had a value of $C_{D,o}$ of 0.0025 which increased to 0.0077 when the first-stage wing was added. The addition of the canard, which had a very small effect on $C_{D,o}$ and the first-stage vertical fins and nacelles increased $C_{D,o}$ to a final value of 0.013 for the complete first stage at $M = 6$. The inclusion of the base drag of the first-stage fuselage increased $C_{D,o}$ appreciably at $M = 3$, but became smaller with increases in Mach number until at $M = 6$ the effect of including the base drag was negligible. The variations in $C_{D,o}$ with Mach number were similar for all the configurations.

Drag-due-to-lift parameters for the complete first stage, presented in figure 9, increased from 0.68 to 1.25 as the test Mach number was increased from 3 to 6. These values compare favorably with those of reference 5 for a similar type wing. Changes in model configuration had little effect on $\frac{\partial C_D}{\partial {C_L}^2}$. Drag-due-to-lift parameters were reasonably constant at lift coefficients up to about 0.12, but show some variation at high lift coefficients resulting from the nonlinearity of the lift curves.

Shown in figure 10 are values of maximum lift-drag ratios for the complete first stage which decreased from about 4.57 to 3.85 as the test Mach number was increased from 3 to 6, and occurred between lift coefficients of about 0.10 and 0.14. Including the base drag of the first-stage fuselage reduced the $(L/D)_{max}$ values of the complete first stage about 17 percent at $M = 3$ and about 6 percent at $M = 4.5$ and had a negligible effect at $M = 6$. At $M = 6$, removing the first-stage fins and nacelles from the first stage increased $(L/D)_{max}$ from 3.85 to 4.8, but removing the canard had little effect on lift-drag ratio. The fuselage alone had an $(L/D)_{max}$ value at $M = 6$ of 4.4, which was higher than that for the complete first stage. The fuselage is a large volume body which is shown in figure 7 to carry considerable lift. Values of $(L/D)_{max}$ for the fuselage alone occurred between lift coefficients of 0.030 and 0.054.

Launch vehicle.- The addition of the complete upper stages to the complete first stage approximately doubled the $C_{D,o}$ values of the first stage at all test Mach numbers (fig. 9). Removal of the second-stage fins and first-stage fins and nacelles caused reductions of as much as 25 percent in $C_{D,o}$, and the maneuver propulsion package was responsible for as much as 12 percent of the $C_{D,o}$ values of the complete launch vehicle. Removing the spacecraft pad, accompanied by lowering the spacecraft 0.3 inch, increased $C_{D,o}$ about 17 percent at $M = 3$, but caused a reduction in $C_{D,o}$ of about 10 percent at $M = 6$. Since the launch vehicle is to be rocket-powered, the large increases in $C_{D,o}$ caused by adding the upper stages to the first stage may not be too important. However, should they become important, better means of integrating the upper stages with the first stage should be sought to eliminate some of the drag penalty. Reference 6 indicates that the drag caused by the upper stages is also high at subsonic and transonic speeds for this vehicle.

Figure 10 shows that the addition of the complete upper stages to the complete first stage reduced $(L/D)_{max}$ values of the first stage more than 20 percent at all test Mach numbers. The $(L/D)_{max}$ values for the complete launch vehicle occurred at lift coefficients appreciably higher than those at which the $(L/D)_{max}$ values for the first stage occurred.

SUMMARY OF RESULTS

An investigation was made in a 2-foot hypersonic facility at the Langley Research Center of a multistage horizontal-take-off reusable launch vehicle. The aerodynamic characteristics of the first-stage reusable booster and the complete launch vehicle with some stage and component effects were determined at Mach numbers of 3, 4.5, and 6, at angles of attack from about -4° to 19°, and at an angle of sideslip of 0°. The principal results may be summarized as follows:

1. For the selected moment reference center, the complete first stage was longitudinally stable at zero lift at a Mach number of 3, but was unstable at Mach numbers of 4.5 and 6. However, the canard produced sizable destabilizing increments, and the first stage without the canard was longitudinally stable at Mach numbers of 3 and 4.5 with marginal stability at a Mach number of 6.

2. Maximum lift-drag ratios for the complete first stage decreased from approximately 4.57 to 3.85 as the test Mach number was increased from 3 to 6. Including the fuselage base drag reduced the maximum lift-drag ratios of the complete first stage about 17 percent at a Mach number of 3 and about 6 percent at a Mach number of 4.5 and had a negligible effect at a Mach number of 6.

3. The addition of the complete upper stages to the complete first stage caused destabilizing increments longitudinally and resulted in increases in drag at zero lift of almost 100 percent at all test Mach numbers.

Langley Research Center,
National Aeronautics and Space Administration,
Langley Station, Hampton, Va., July 13, 1964.

1. Pierpont, P. Kenneth: Transonic Stability of a Preliminary Vertical-Take-Off Launch Configuration With a Horizontal-Landing Recoverable Booster. NASA TM X-689, 1962.

2. Pierpont, P. Kenneth: Transonic Longitudinal and Lateral Aerodynamic Characteristics of a Preliminary Concept of a First-Stage Horizontal-Take-Off-and-Horizontal-Landing Recoverable Booster With a 70° Delta Wing. NASA TM X-691, 1962.

3. Pierpont, P. Kenneth: Transonic Aerodynamic Characteristics of a Horizontal-Take-Off-and-Horizontal-Landing Recoverable-Booster Concept With Upper Stages Arranged in Parallel. NASA TM X-696, 1962.

4. Clark, Larry R.; and Pierpont, P. Kenneth: Hypersonic Aerodynamic Characteristics of Preliminary Vertical-Take-Off Launch Configurations With a Horizontal-Landing Reusable Booster. NASA TM X-887, 1963.

5. Clark, Larry R.; and Pierpont, P. Kenneth: Spacecraft and Stage-Geometry Effects on the Hypersonic Characteristics of a Horizontal-Take-Off Reusable Booster. NASA TM X-900, 1963.

6. Clark, Larry R.; and Pierpont, P. Kenneth: Transonic Characteristics of a Hydrogen-Fueled Multistage Horizontal-Take-Off Reusable Launch Vehicle. NASA TM X-1008, 1964.

7. Stokes, George M.: Description of a 2-Foot Hypersonic Facility at the Langley Research Center. NASA TN D-939, 1961.

TABLE I.- GEOMETRIC DESIGN CHARACTERISTICS OF THE MODEL

First stage:	
Fuselage:	
Length, in.	23.760
Maximum diameter, in.	2.524
Maximum height, in.	1.922
Nose radius, in.	0.096
Base area, sq in.	4.164
Wing:	
Total area, sq in.	63.360
Exposed area, sq in.	34.432
Span, in.	9.600
Root chord, in.	13.200
Tip chord, in.	0
Maximum thickness, percent chord	5.00
Leading-edge sweep angle, deg	70.00
Leading-edge radius, in.	0.024
Mean aerodynamic chord, in.	8.800
Moment reference center, percent $\bar{c}$	15
Moment reference center, in. from base	7.480
Vertical fins:	
Area of each fin (exposed), sq in.	4.608
Height (exposed), in.	1.152
Root chord, in.	2.664
Tip chord, in.	1.332
Leading-edge sweep angle, deg	60.00
Trailing-edge sweep angle, deg	29.92
Leading-edge radius, in.	0.024
Wing nacelles:	
Length, in.	3.982
Maximum diameter, in.	0.576
Fineness ratio	6.910
Nose radius, in.	0.096
Canard:	
Total area, sq in.	12.804
Exposed area, sq in.	4.478
Span, in.	4.320
Root chord, in.	5.928
Tip chord, in.	0
Maximum thickness, percent chord	5
Leading-edge sweep angle, deg	70.00
Leading-edge radius, in.	0.024

TABLE I.- GEOMETRIC DESIGN CHARACTERISTICS OF THE MODEL - Concluded

Second stage:	
Fuselage:	
Length, in.	9.600
Diameter, in.	1.280
Base area, sq in.	1.464
Wing:	
Total area, sq in.	27.072
Exposed area, sq in.	18.612
Span, in.	5.760
Root chord, in.	7.068
Tip chord, in.	2.311
Maximum thickness, percent chord	2.800
Leading-edge sweep angle, deg	58.75
Leading-edge radius, in.	0.024
Vertical fins:	
Area of each fin (exposed), sq in.	2.276
Height, in.	1.249
Root chord, in.	2.580
Tip chord, in.	1.332
Leading-edge sweep angle, deg	60.00
Trailing-edge sweep angle, deg	29.92
Leading-edge radius, in.	0.024
Spacecraft:	
Fuselage:	
Length, including interstage, in.	6.048
Diameter, in.	0.672
Interstage base diameter, in.	1.280
Interstage included angle, deg	35.20
Length of nose cone, in.	0.857
Nose-cone included angle, deg	35.00
Nose radius, in.	0.096
Wing:	
Total area, sq in.	8.527
Exposed area, sq in. (top surface)	5.347
Exposed area, sq in. (bottom surface)	3.064
Span, in.	2.506
Root chord, in.	5.296
Tip chord, in.	1.589
Maximum thickness, percent chord	5
Leading-edge sweep angle, deg	72.50
Leading-edge radius, in.	0.024
Wing nose radius, in.	0.096
Vertical fins:	
Area, sq in.	0.866
Height, in.	0.858
Root chord, in.	1.589
Tip chord, in.	0.480
Maximum thickness, percent chord	5
Leading-edge sweep angle, deg	55.00
Leading-edge radius, in.	0.024
Lateral inclination angle, deg	3.00
Pad:	
Length, in.	6.048
Maximum width, in.	1.280
Nose radius, in.	0.096
Wedge included angle, deg	72.50
Maneuver propulsion package:	
Length, in.	2.880
Diameter, in.	1.280

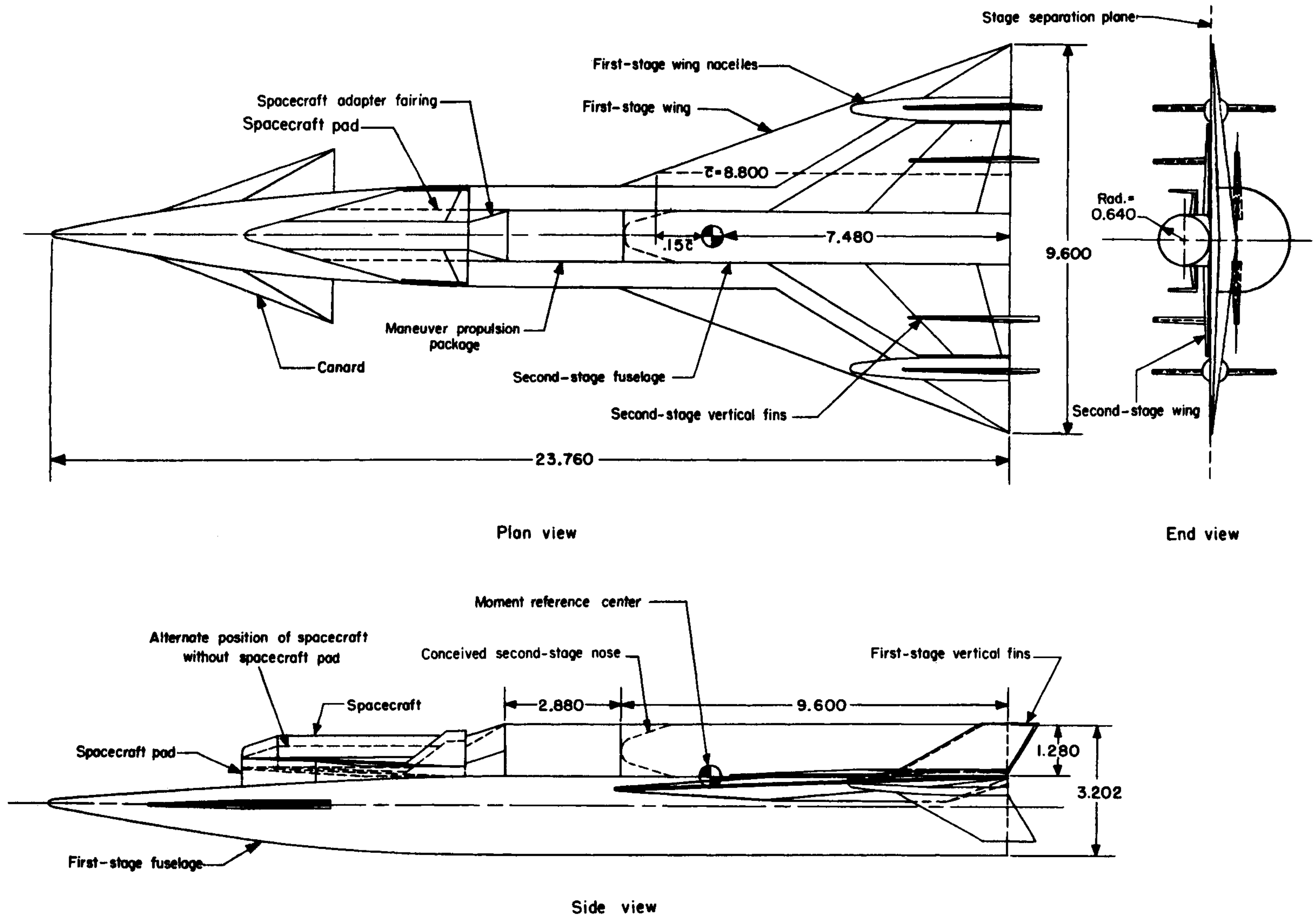

(a) General arrangement of the launch vehicle.

Figure 1.- Arrangement and geometric details of a three-stage horizontal-take-off reusable booster system. All linear design dimensions are in inches.

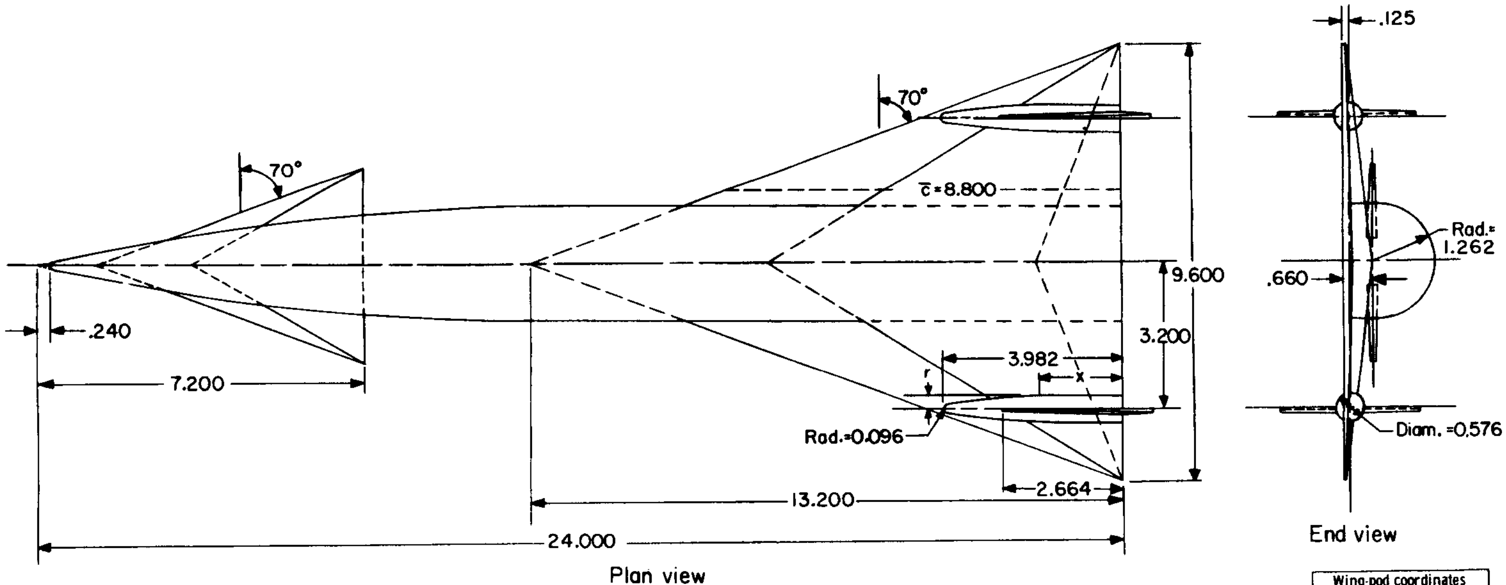

Wing-pod coordinates	
x	r
0	0.288
1.722	.288
2.222	.278
2.722	.247
3.222	.196

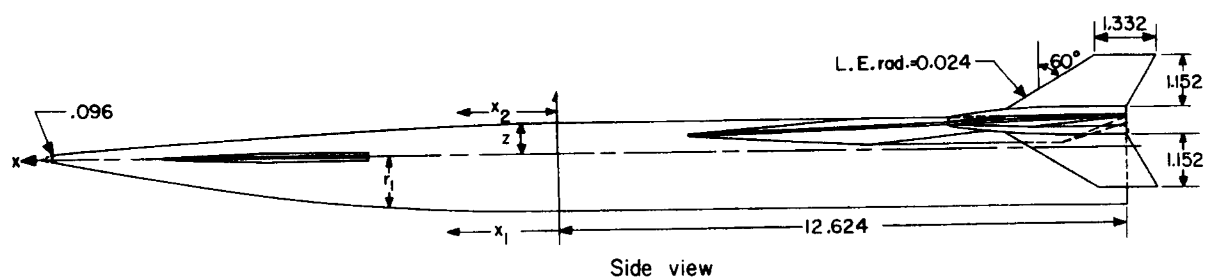

Fuselage coordinates			
x_1	r_1	x_2	z
0	1.262	0	0.660
1.000	1.253	1.376	.618
1.999	1.223	2.376	.587
3.000	1.114	3.376	.553
4.000	1.106	4.376	.517
5.000	1.018	4.776	.479
6.000	.910	6.376	.438
7.000	.783	7.376	.391
8.000	.636	8.376	.338
9.000	.470	9.376	.277
10.000	.284	9.876	.239
11.000	.079	10.376	.195
11.376	0	10.626	.169
		10.876	.138
		11.126	.098
		11.376	0

(b) First-stage reusable booster.

Figure 1.- Continued.

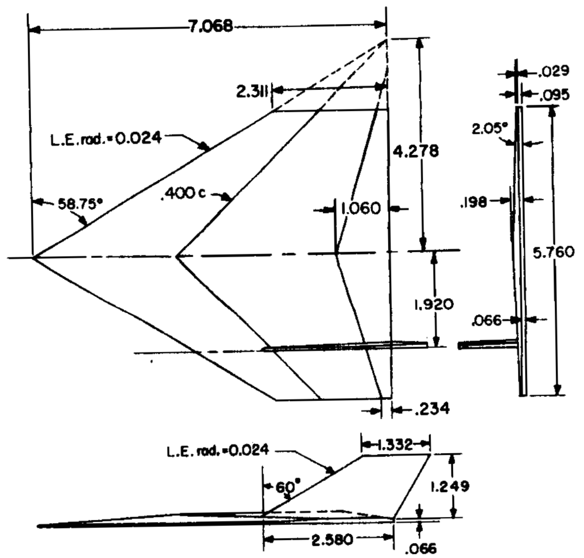

Second-stage wing

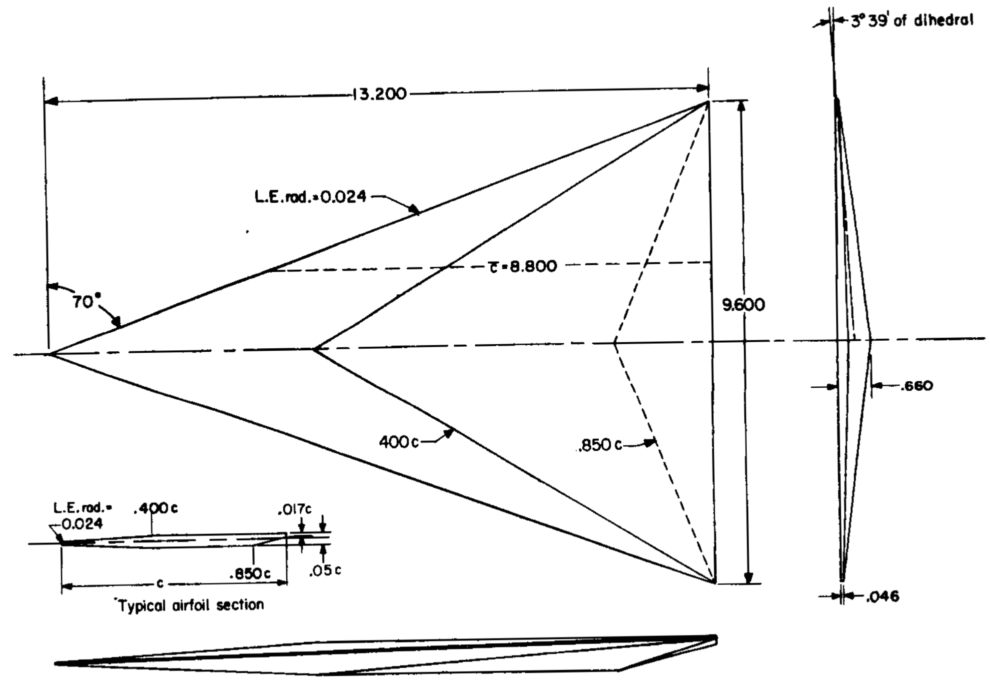

First-stage wing

(c) Details of first-stage wing and second-stage wing and fins.

Figure 1.- Continued.

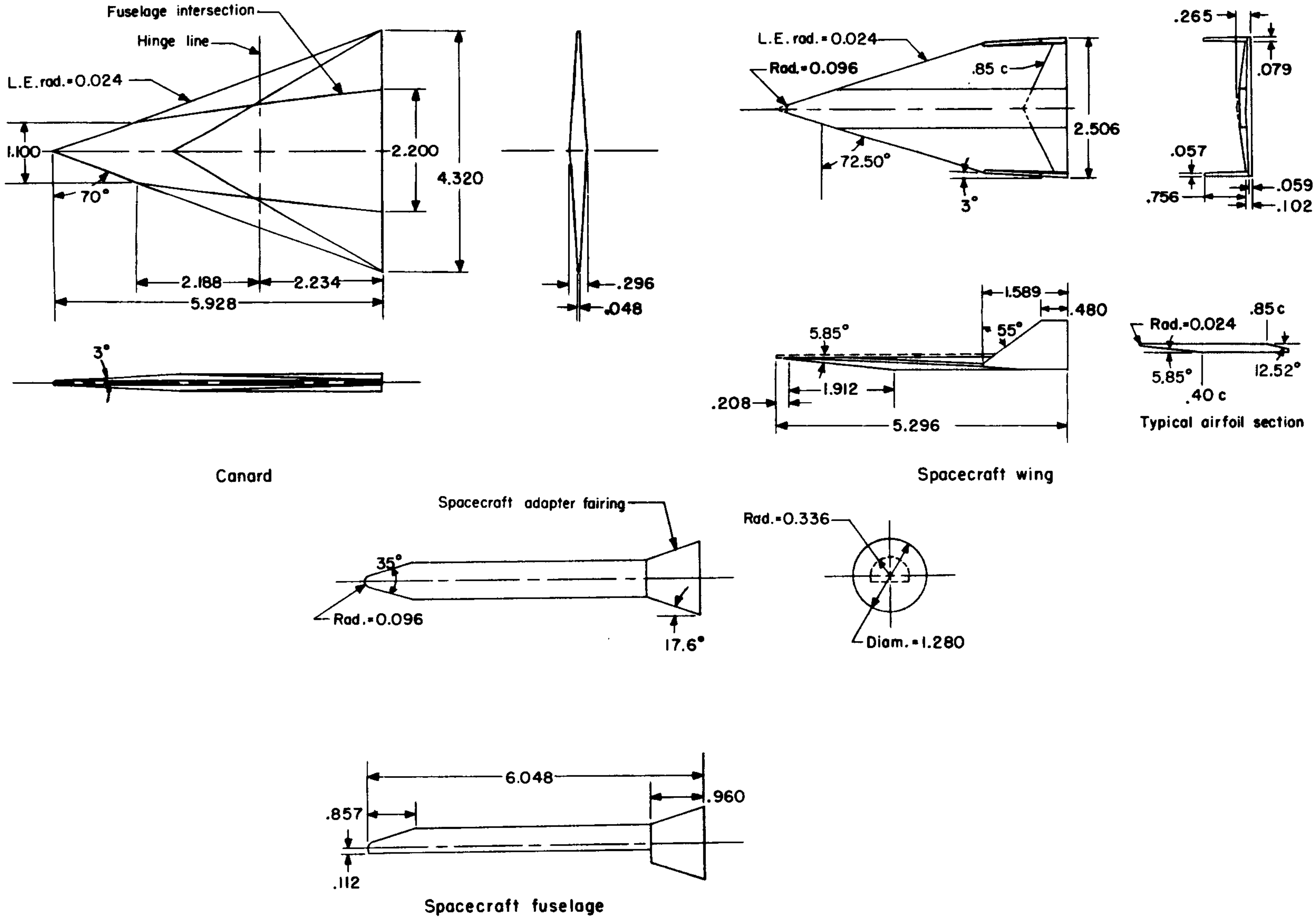

(d) Details of canard and spacecraft.

Figure 1.- Concluded.

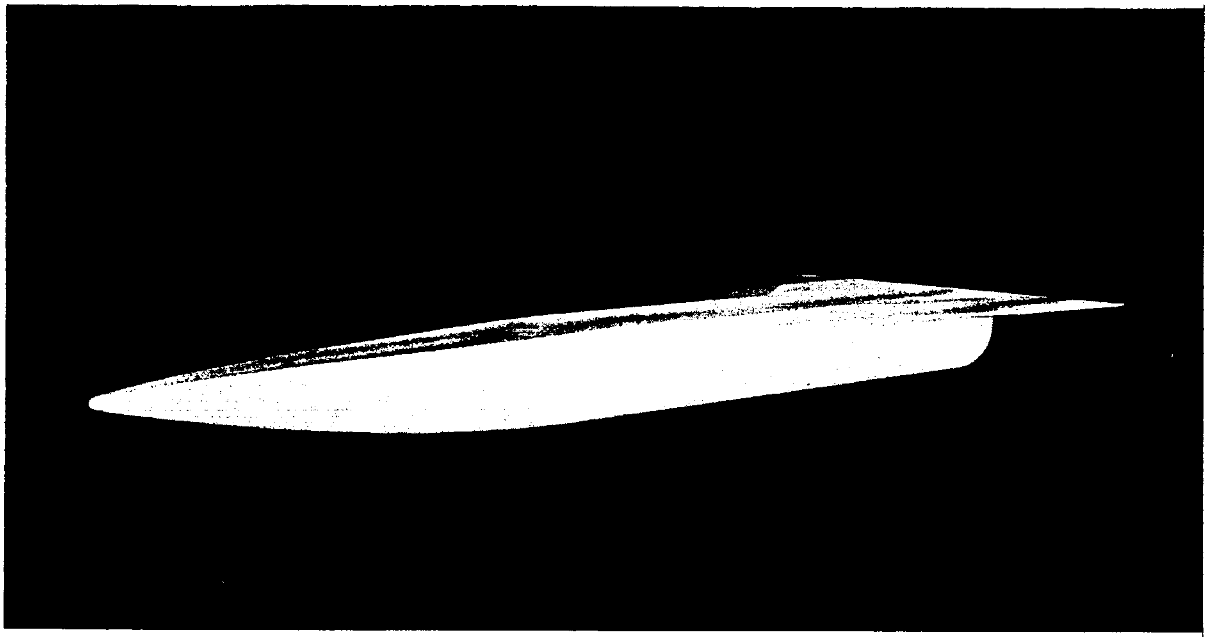

(a) First-stage wing-fuselage combination. L-63-6494

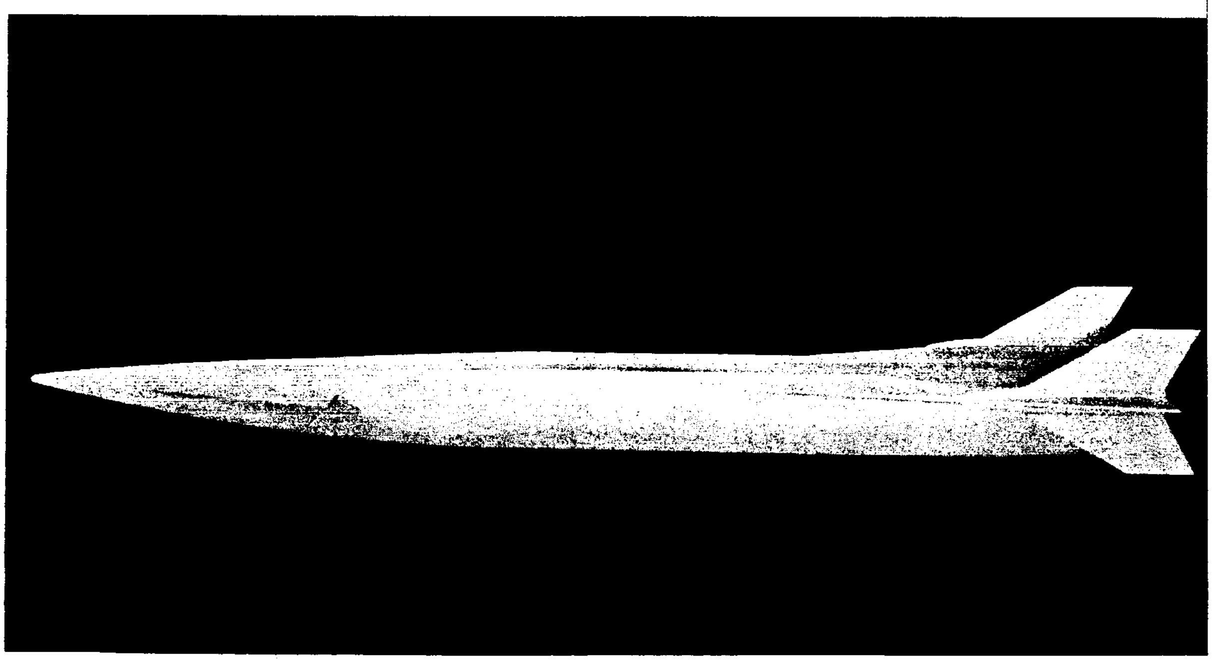

(b) Complete first-stage reusable booster. L-63-6483

Figure 2.- Photographs of model configurations.

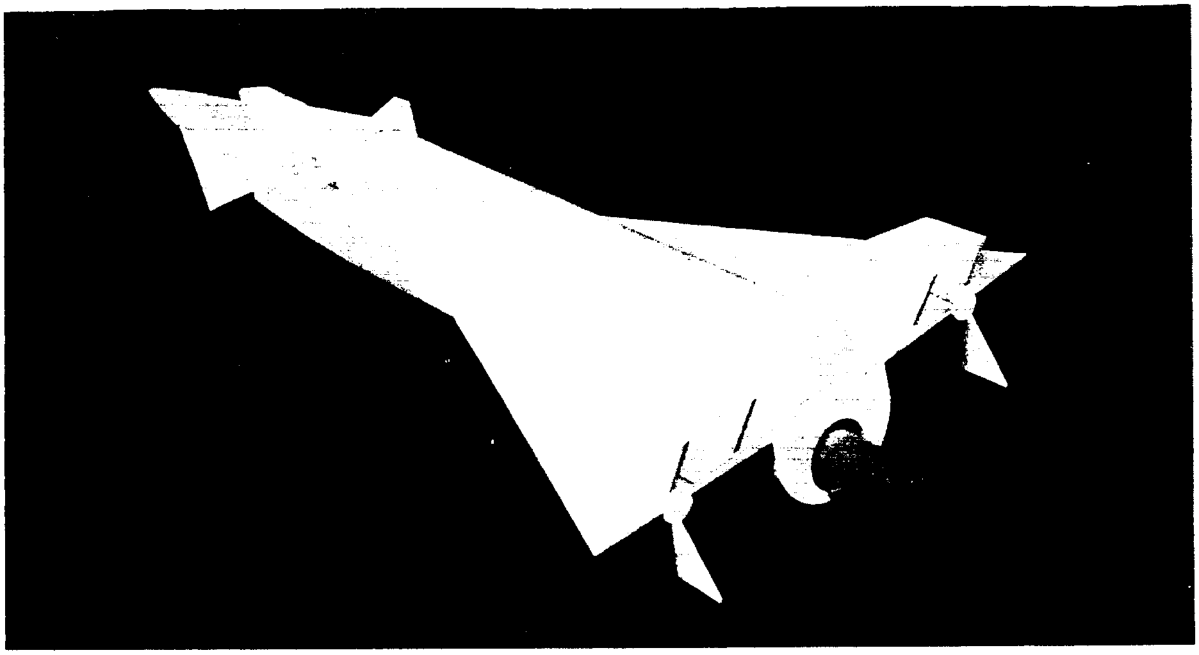

(c) Complete launch vehicle. L-63-6489

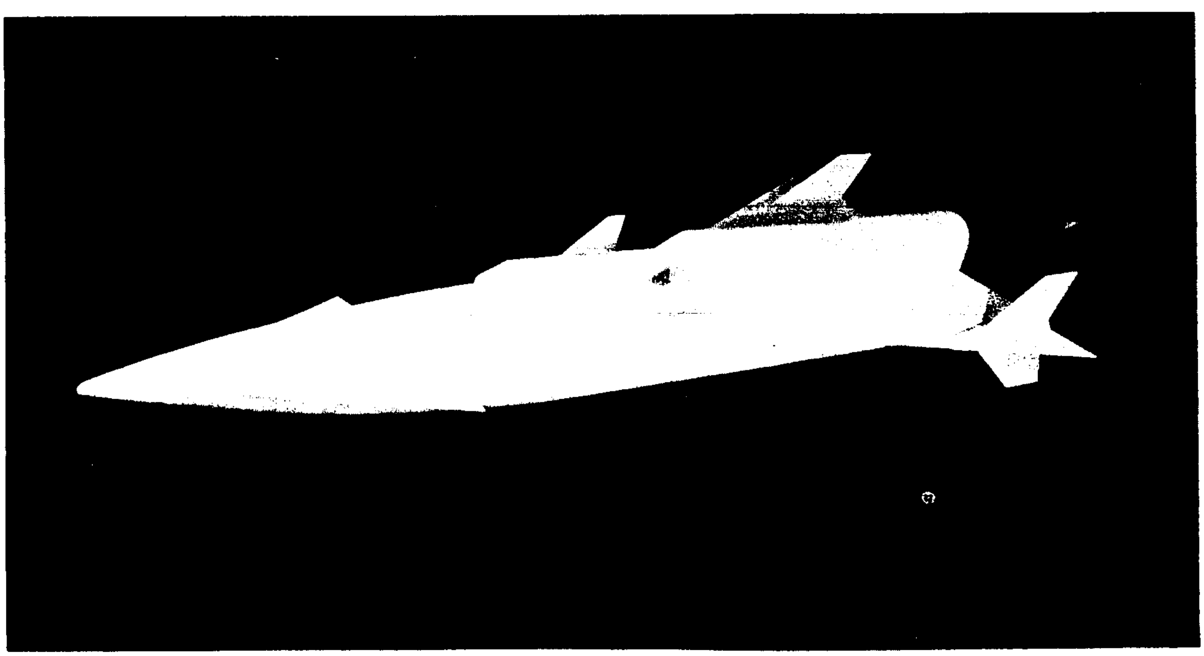

(d) Launch vehicle without the maneuver propulsion package. L-63-6481

Figure 2.- Concluded.

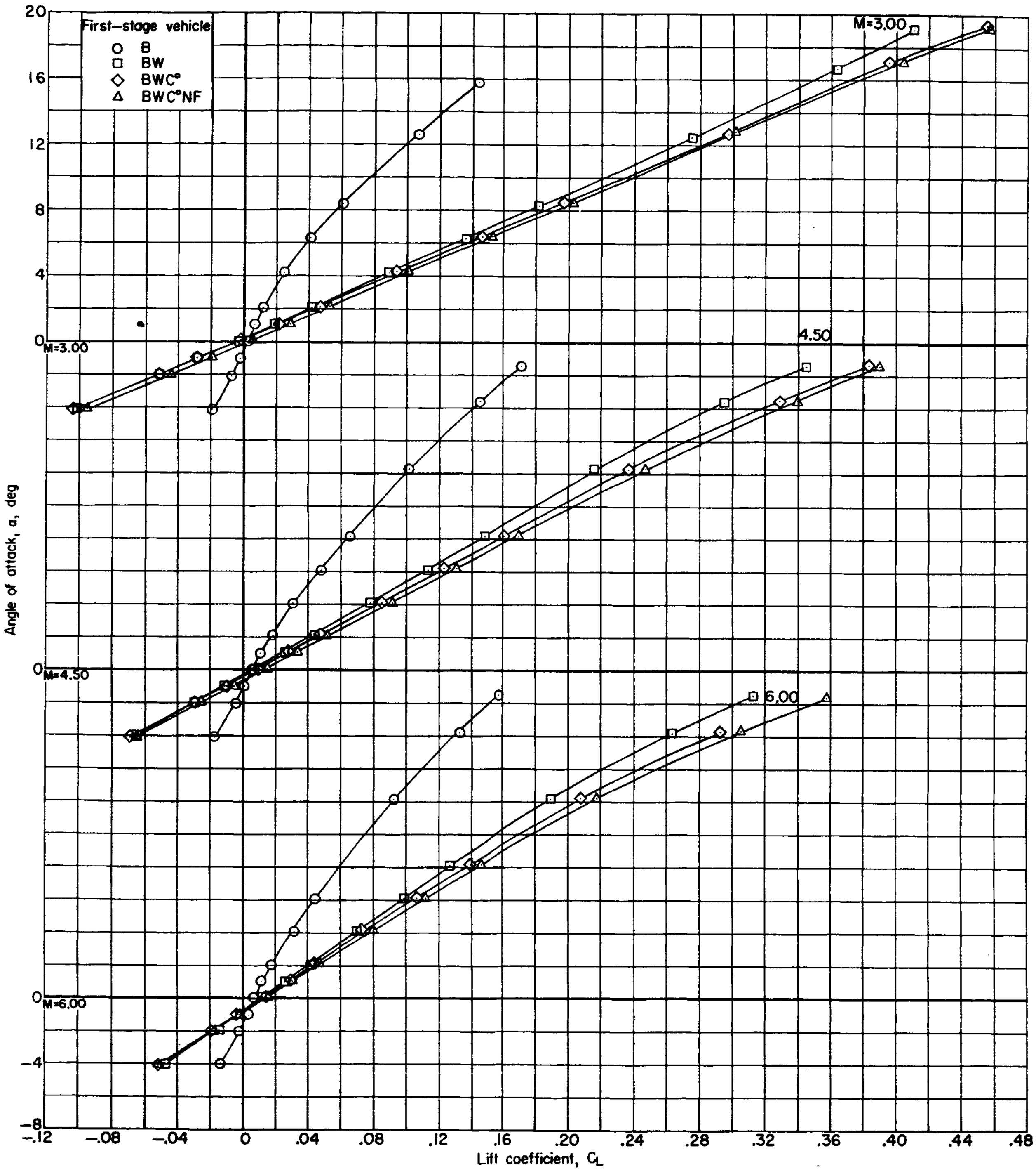

(a) Variation of angle of attack with lift coefficient.

Figure 3.- Longitudinal aerodynamic characteristics for the first-stage reusable booster with its several modifications.

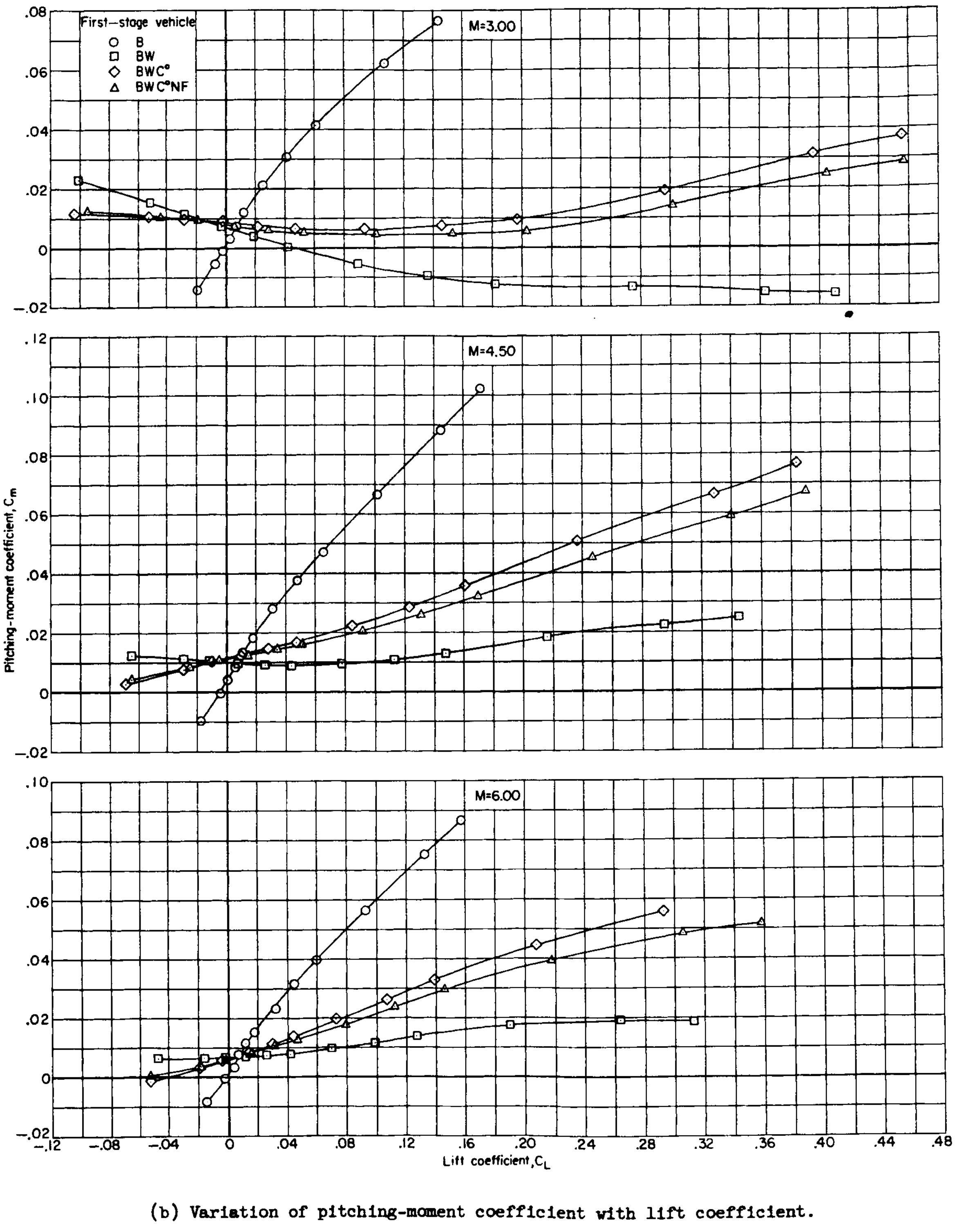

(b) Variation of pitching-moment coefficient with lift coefficient.

Figure 3.- Continued.

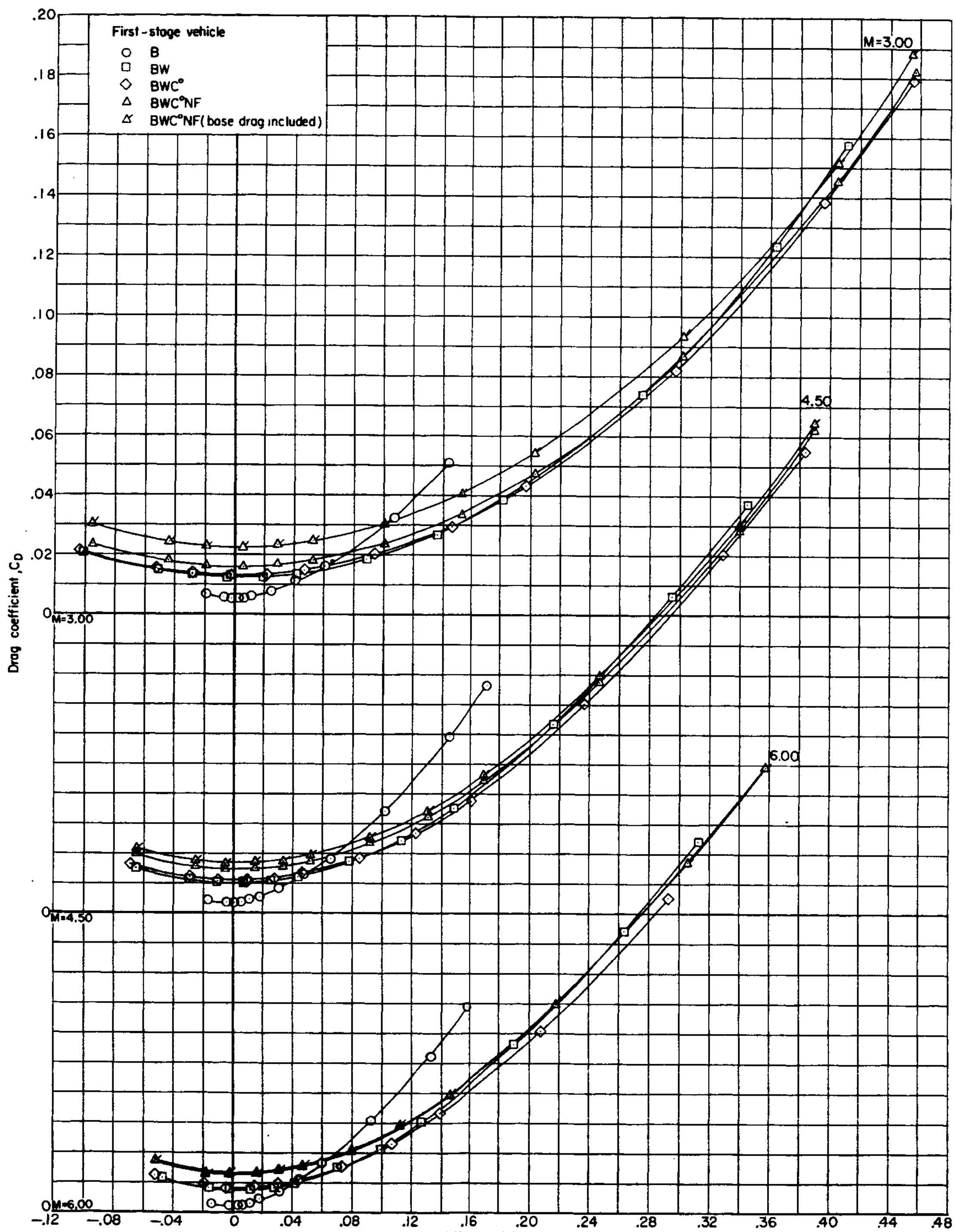

(c) Variation of drag coefficient with lift coefficient.

Figure 3.- Continued.

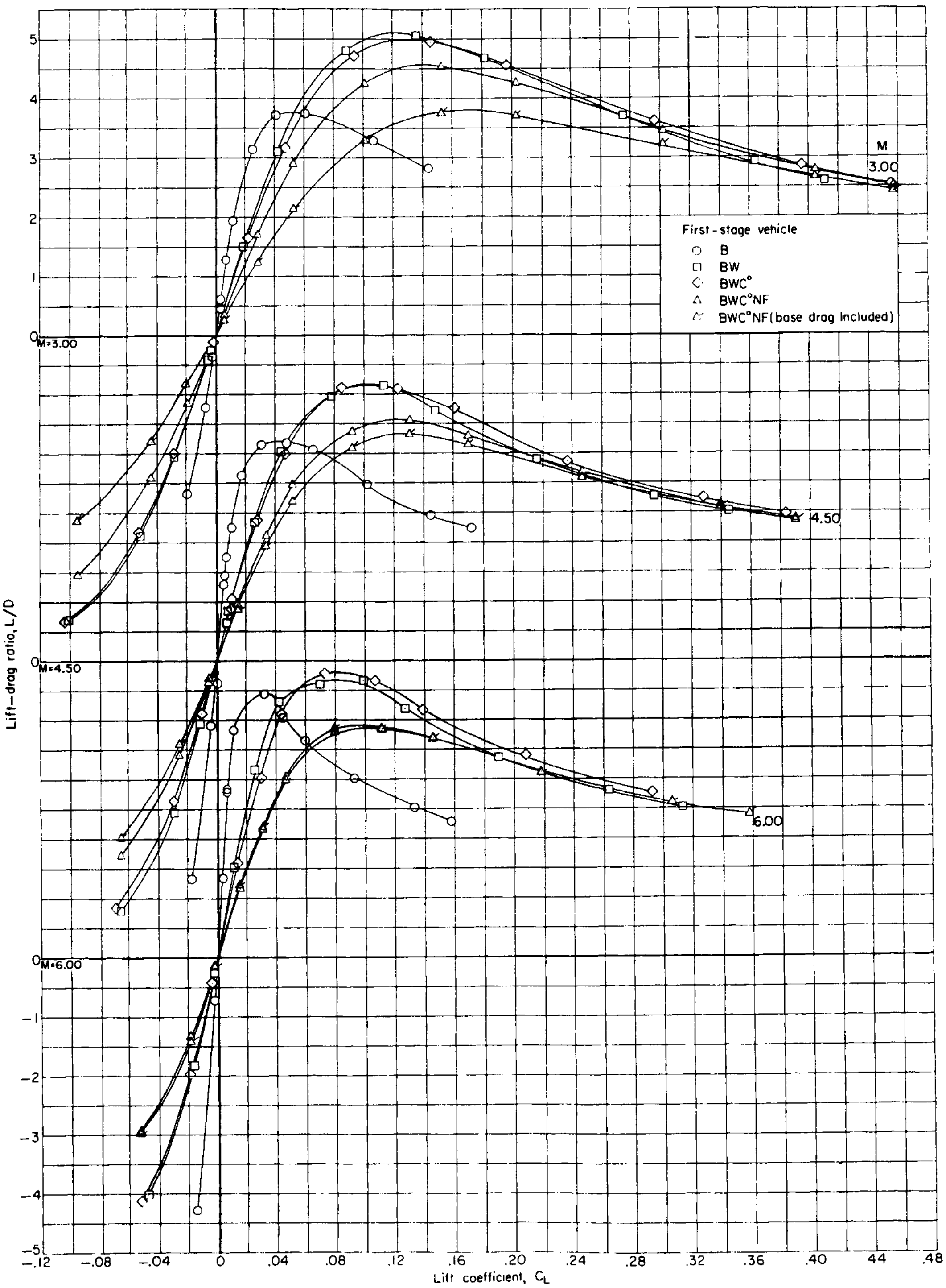

(d) Variation of lift-drag ratio with lift coefficient.

Figure 3.- Concluded.

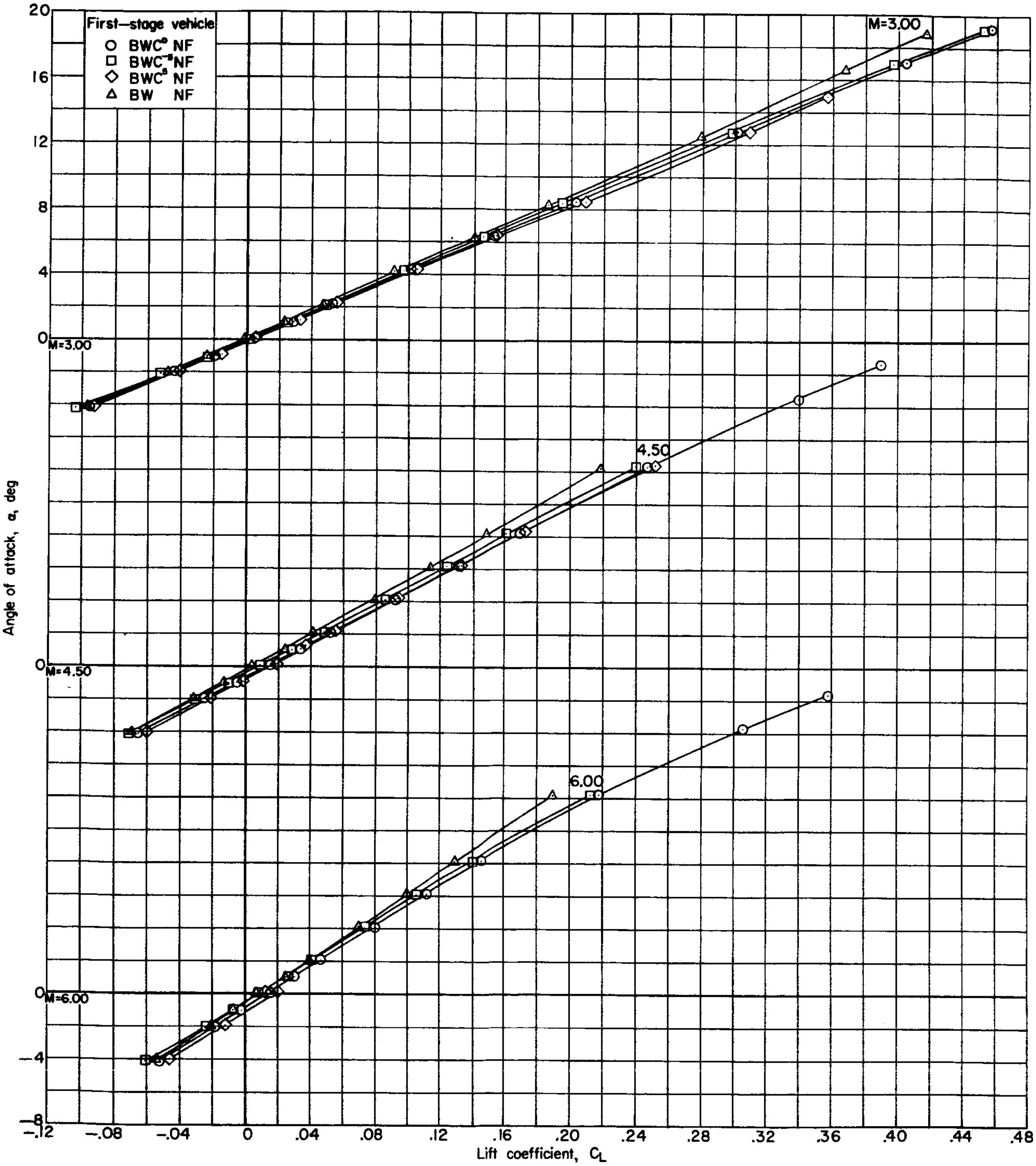

(a) Variation of angle of attack with lift coefficient.

Figure 4.- Longitudinal aerodynamic characteristics for the first-stage reusable booster with the effects of the canard.

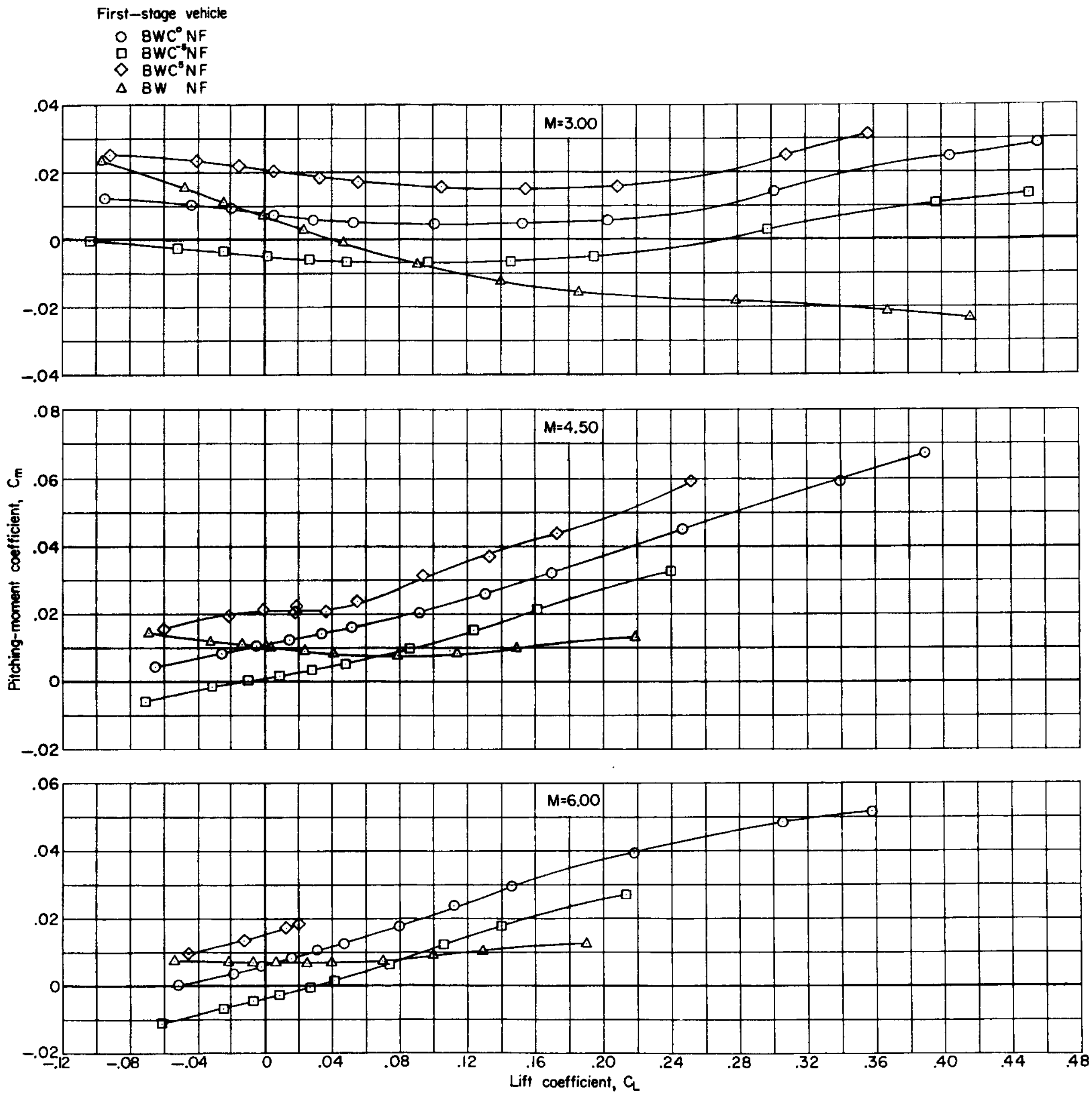

(b) Variation of pitching-moment coefficient with lift coefficient.

Figure 4.- Continued.

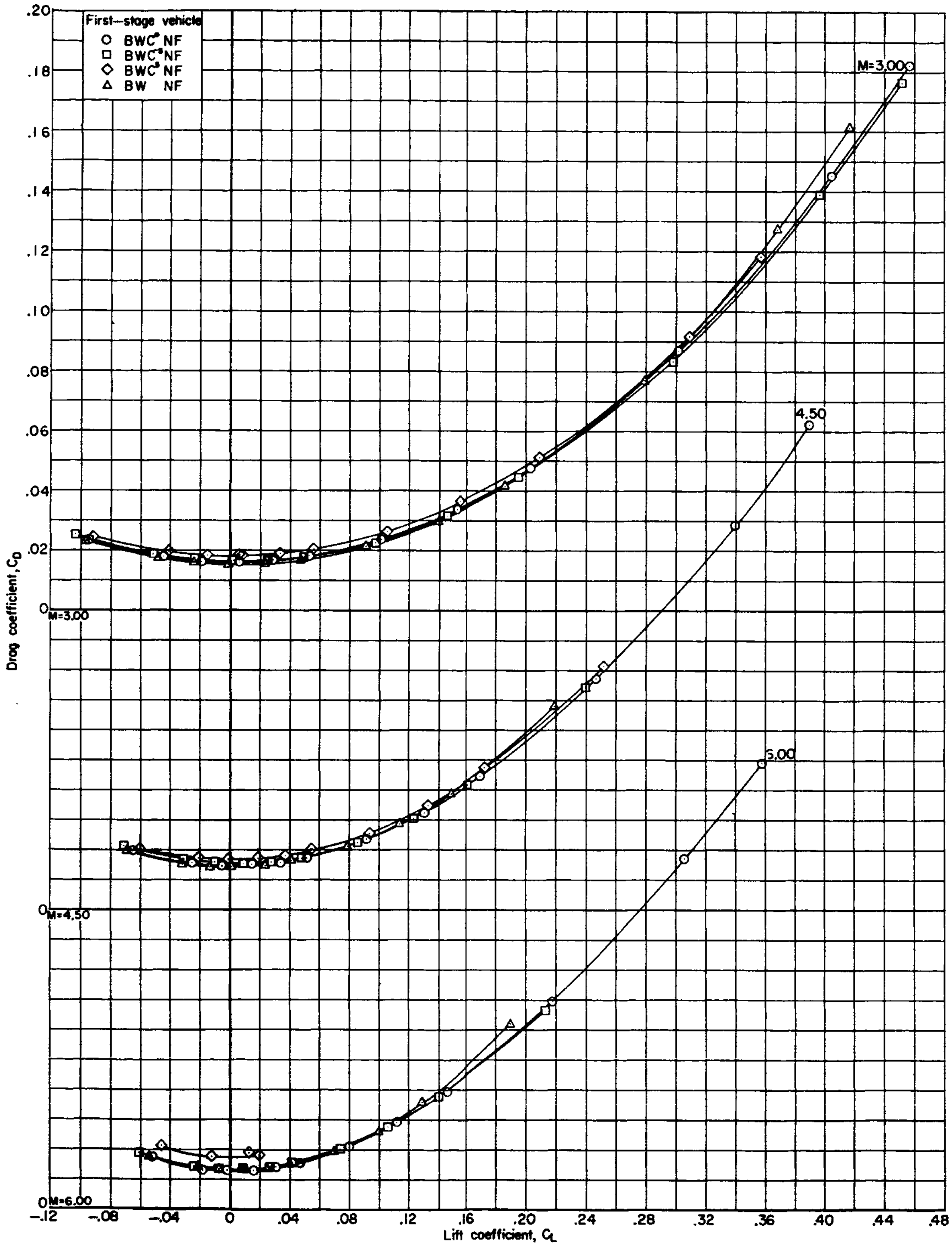

(c) Variation of drag coefficient with lift coefficient.

Figure 4.- Continued.

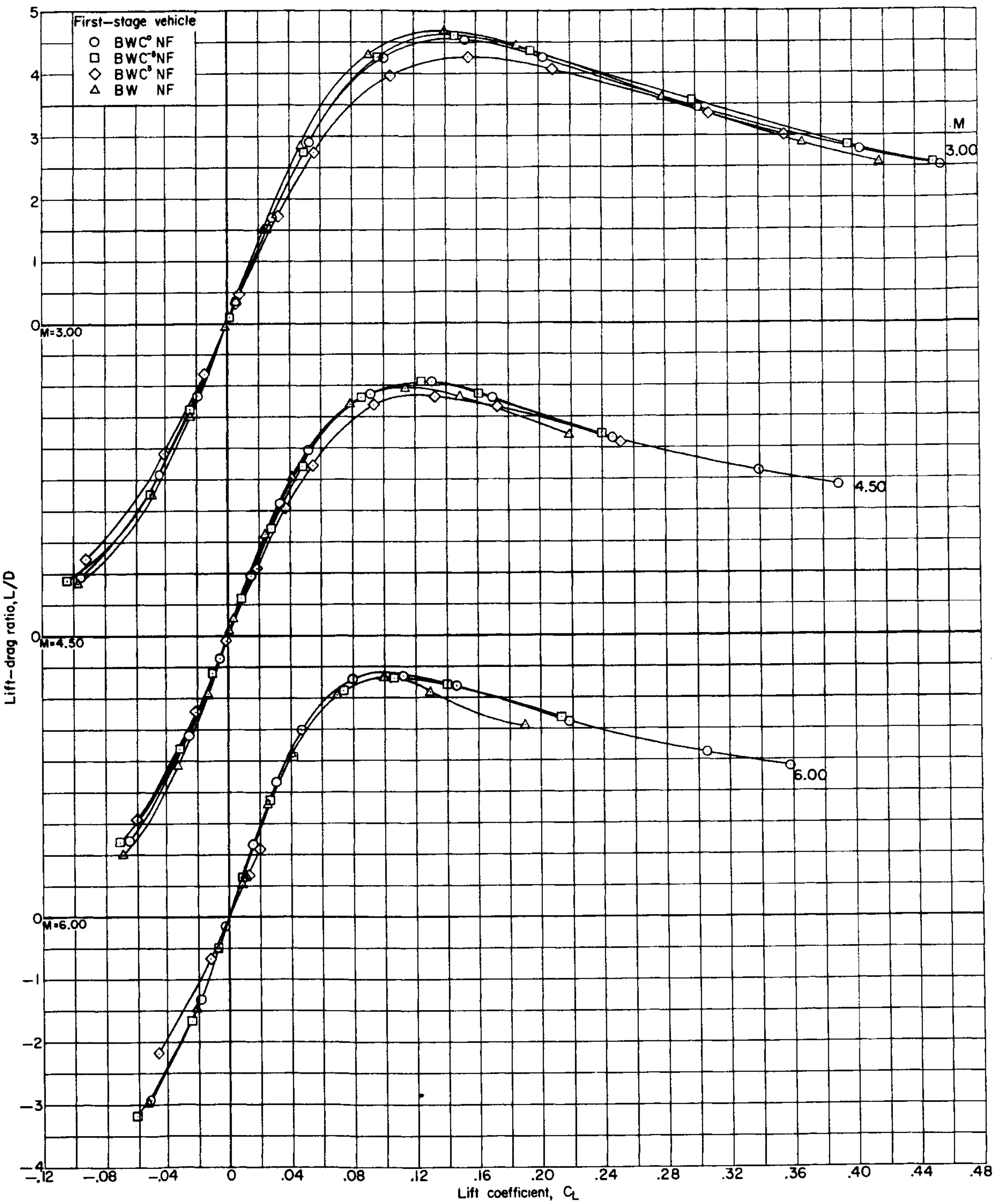

(d) Variation of lift-drag ratio with lift coefficient.

Figure 4.- Concluded.

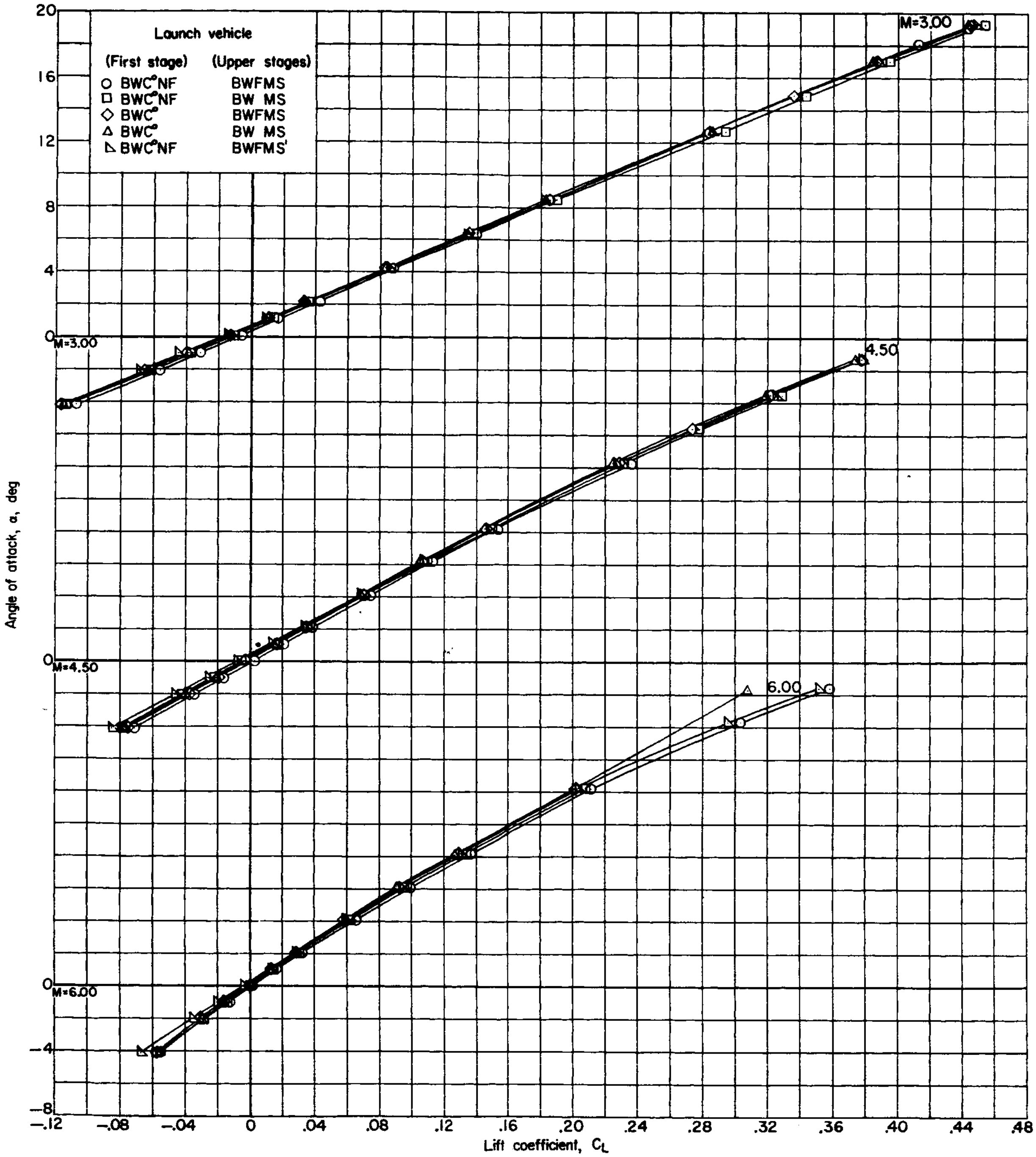

(a) Variation of angle of attack with lift coefficient.

Figure 5.- Longitudinal aerodynamic characteristics for the basic launch vehicle with the effects of the second-stage vertical fins, the first-stage vertical fins and nacelles, and the spacecraft pad.

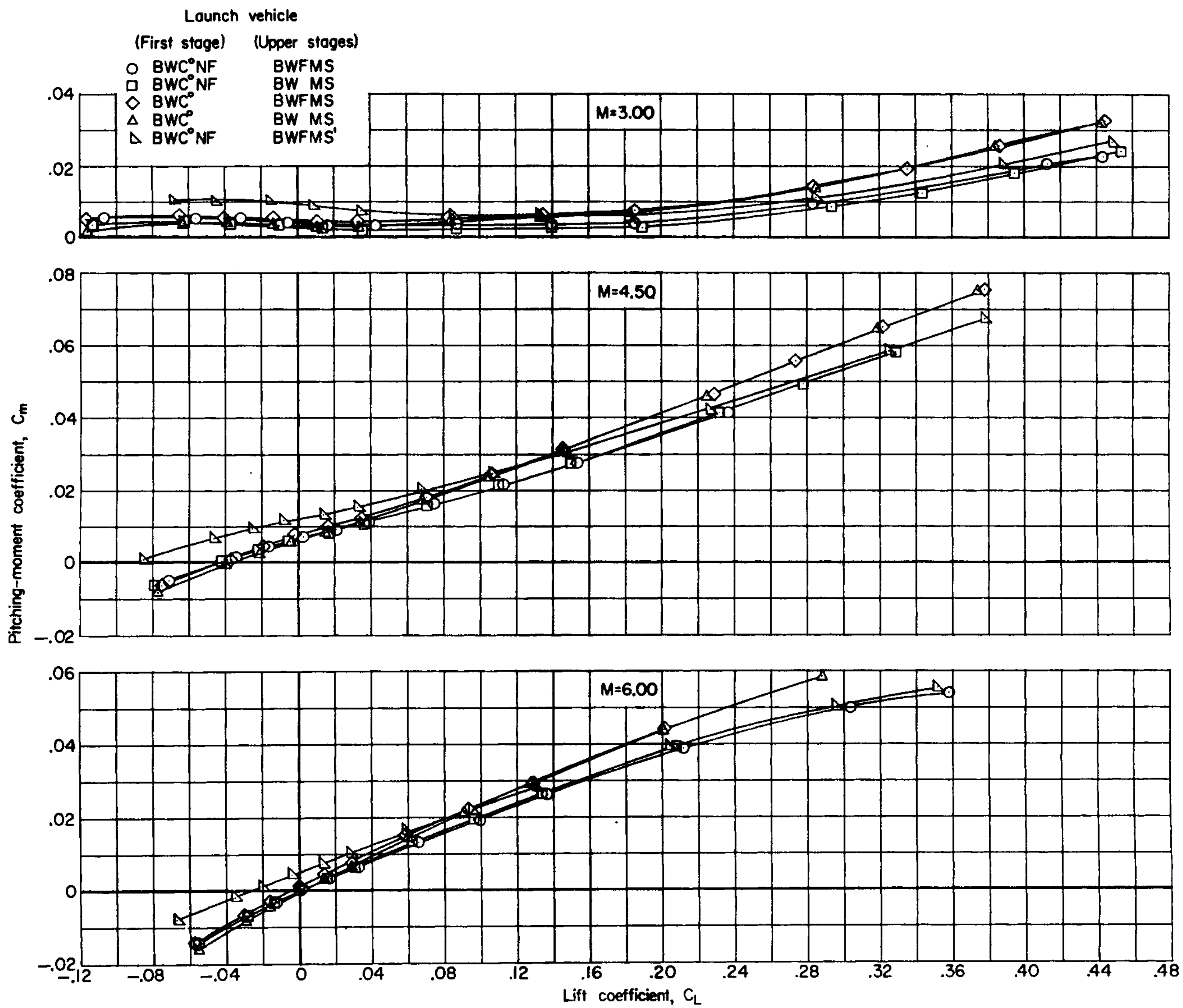

(b) Variation of pitching-moment coefficient with lift coefficient.

Figure 5.- Continued.

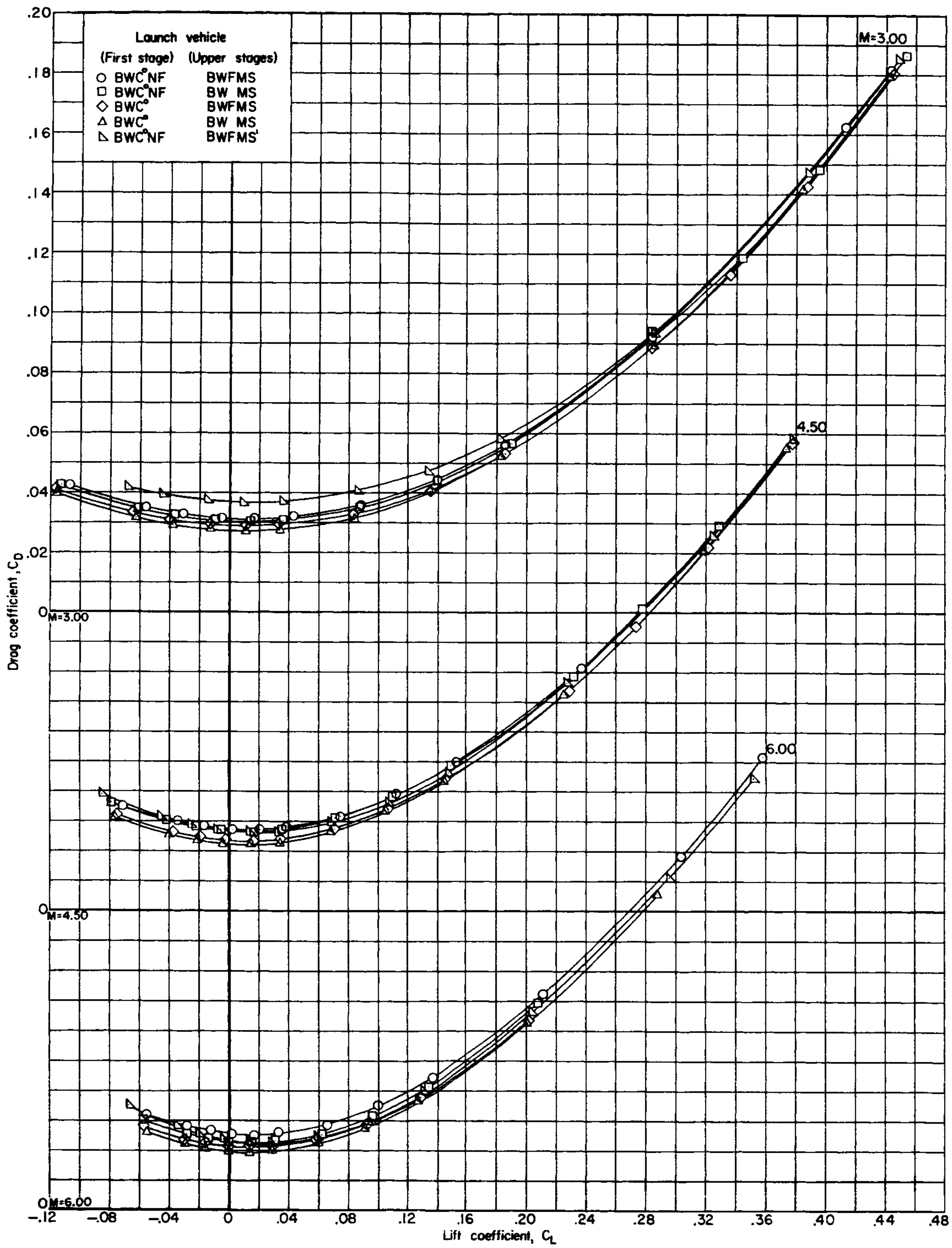

(c) Variation of drag coefficient with lift coefficient.

Figure 5.- Continued.

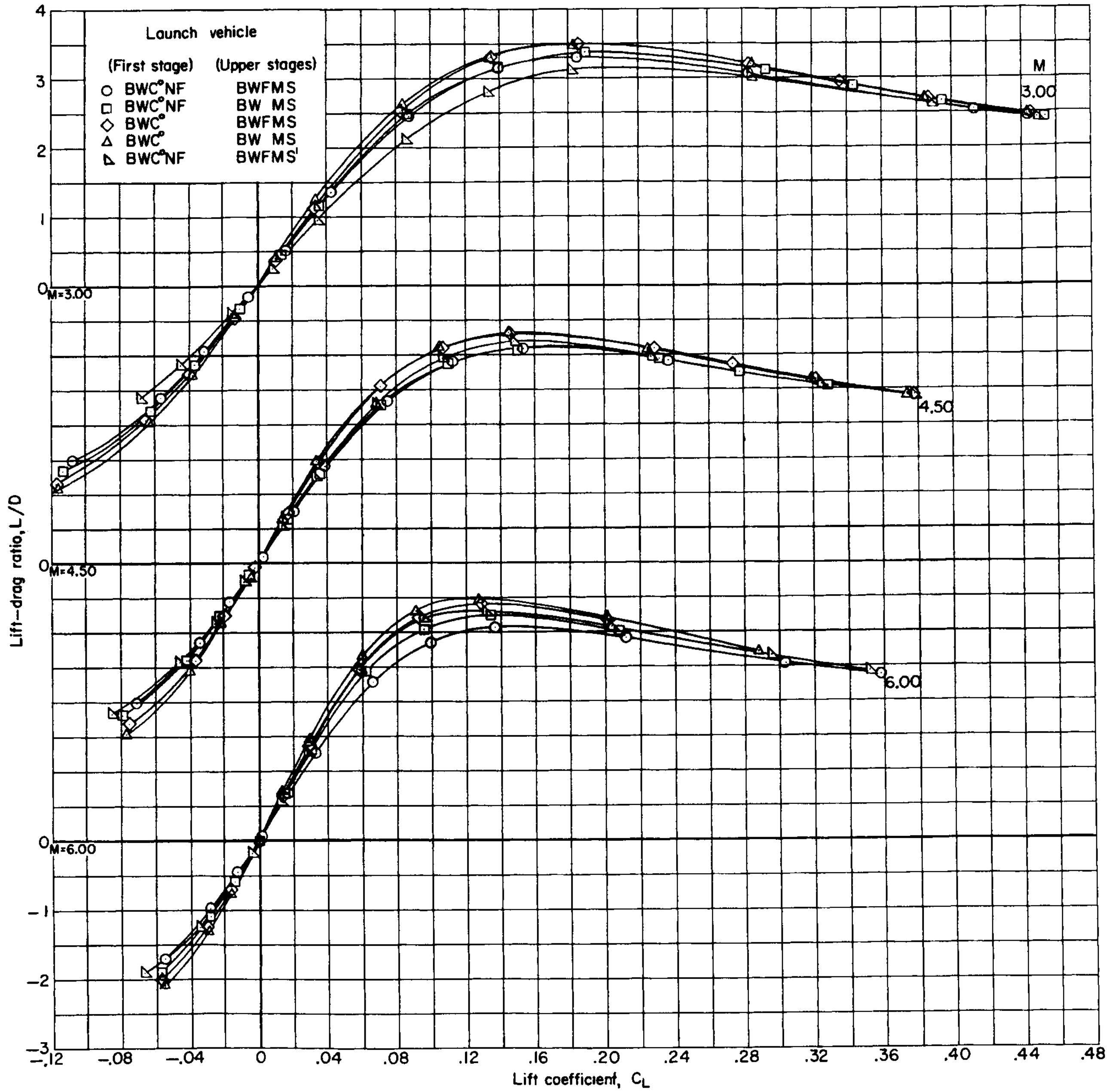

(d) Variation of lift-drag ratio with lift coefficient.

Figure 5.- Concluded.

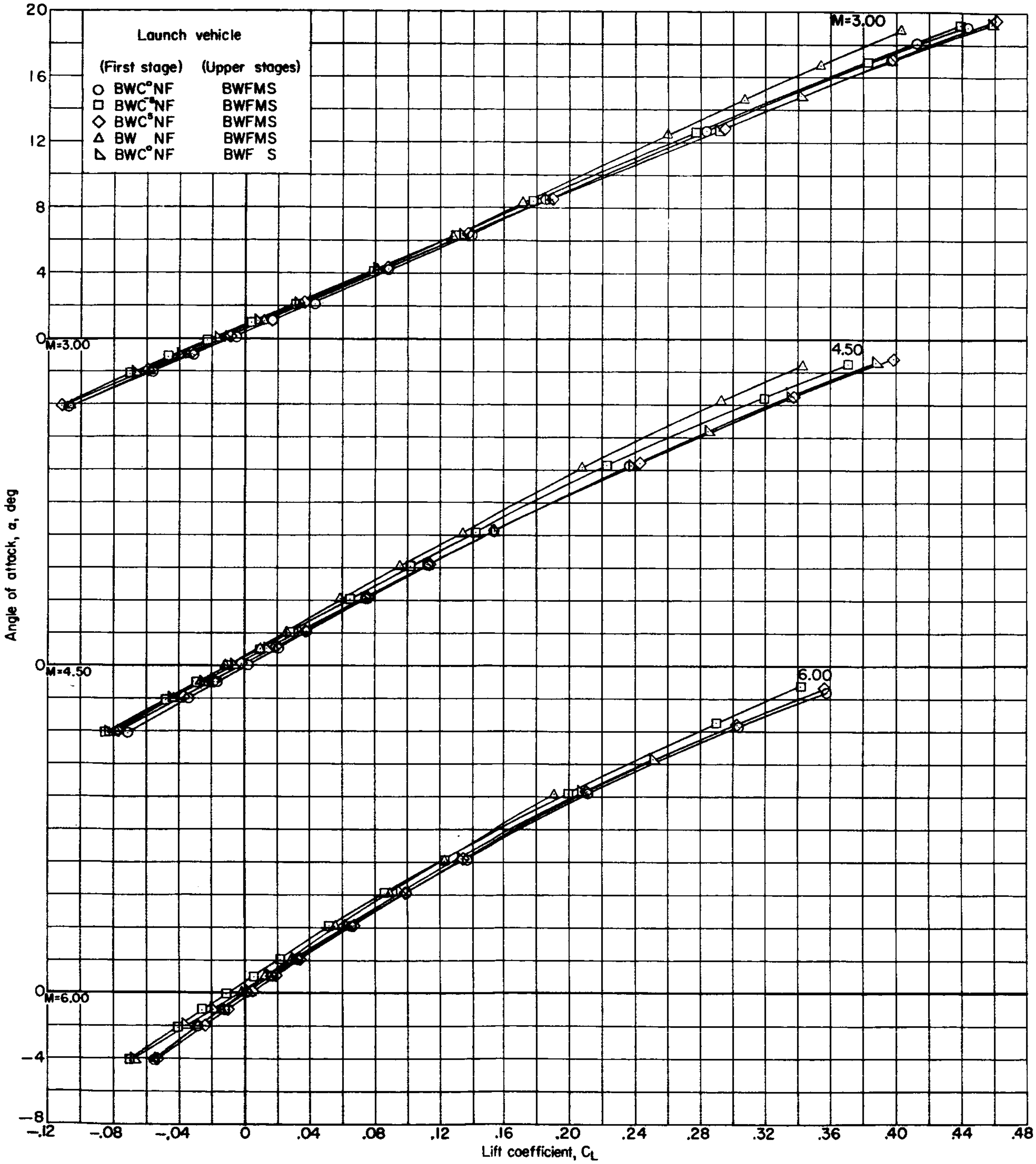

(a) Variation of angle of attack with lift coefficient.

Figure 6.- Longitudinal aerodynamic characteristics for the basic launch vehicle with the effects of the canard and the maneuver propulsion package.

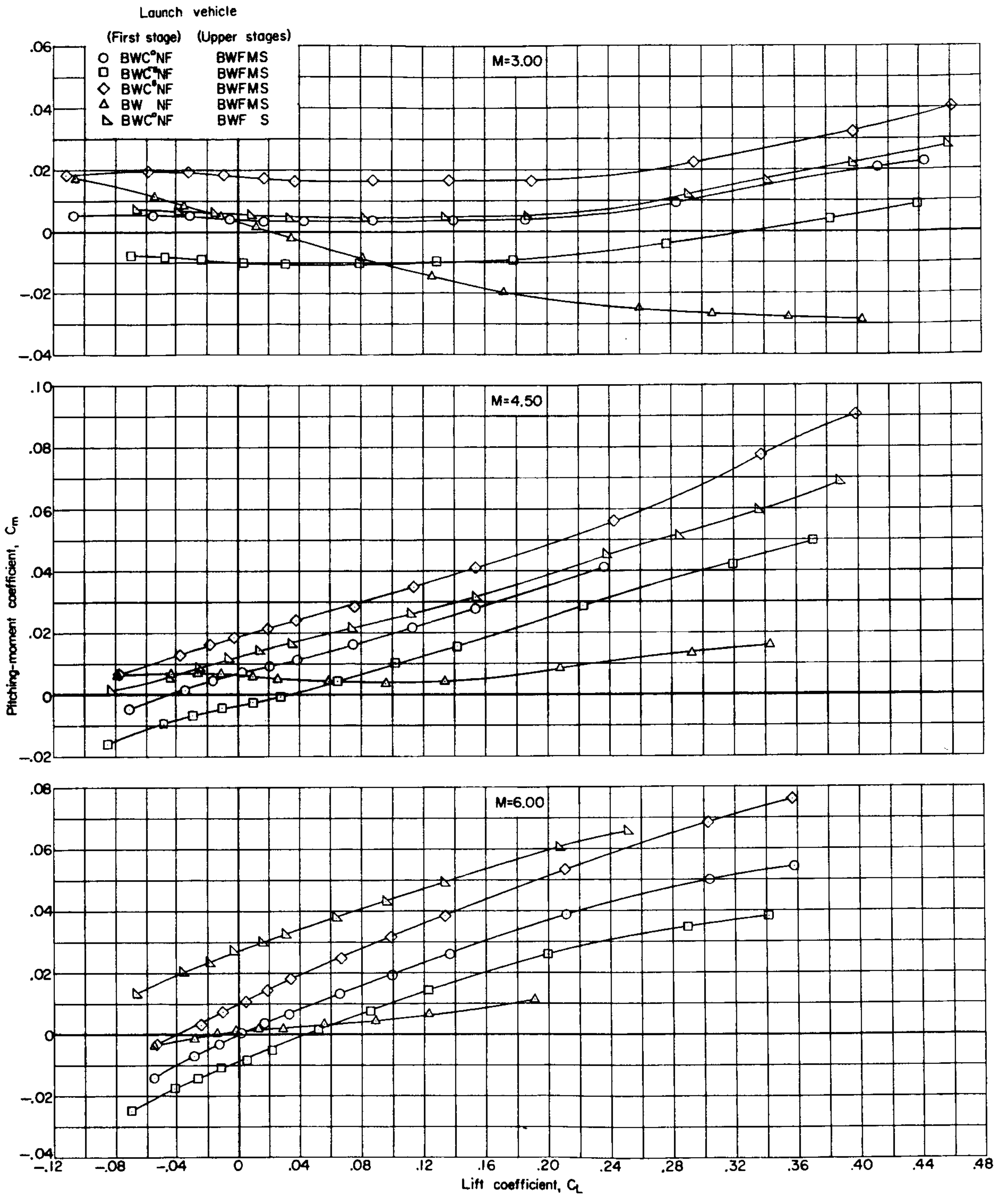

(b) Variation of pitching-moment coefficient with lift coefficient.

Figure 6.- Continued.

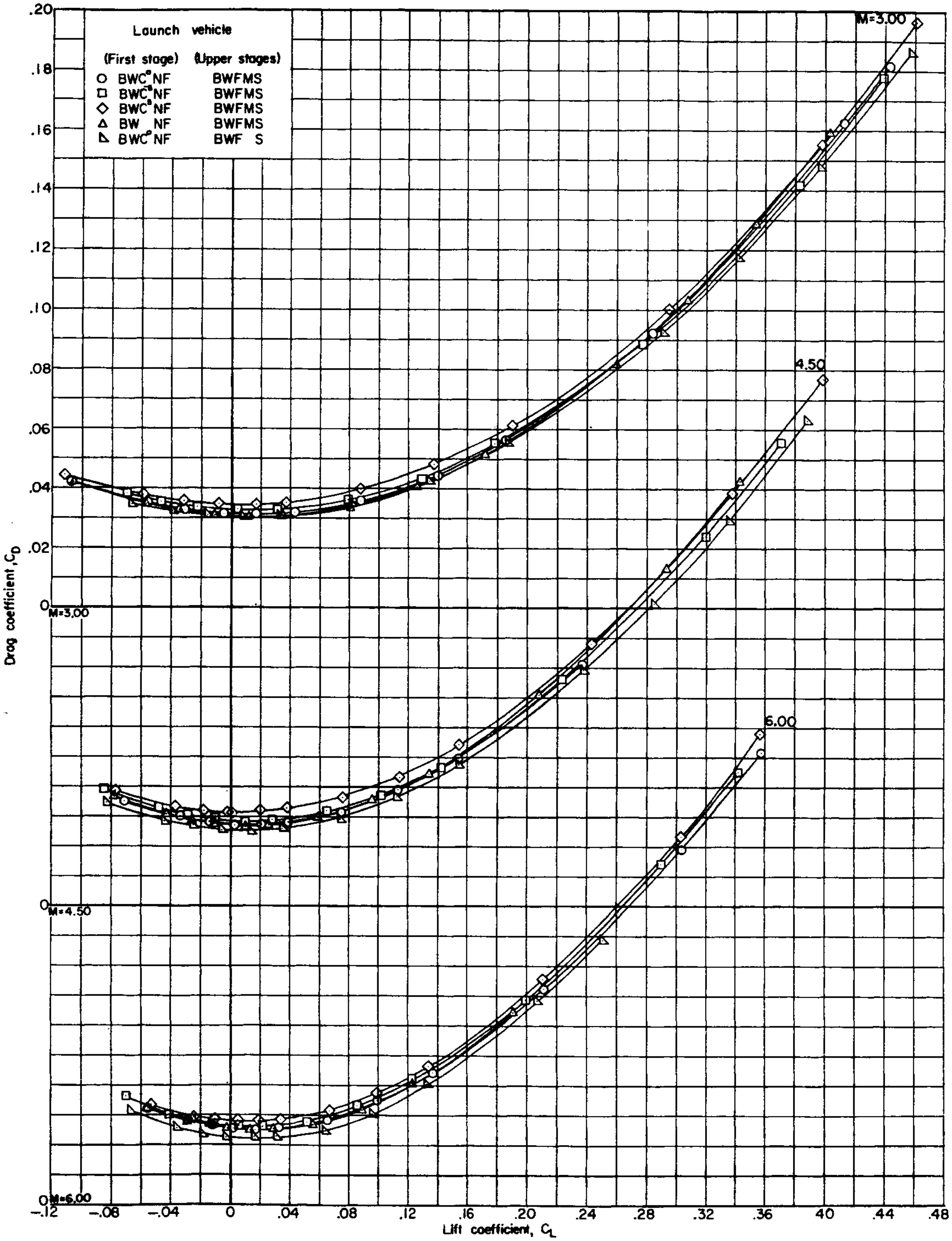

(c) Variation of drag coefficient with lift coefficient.

Figure 6.- Continued.

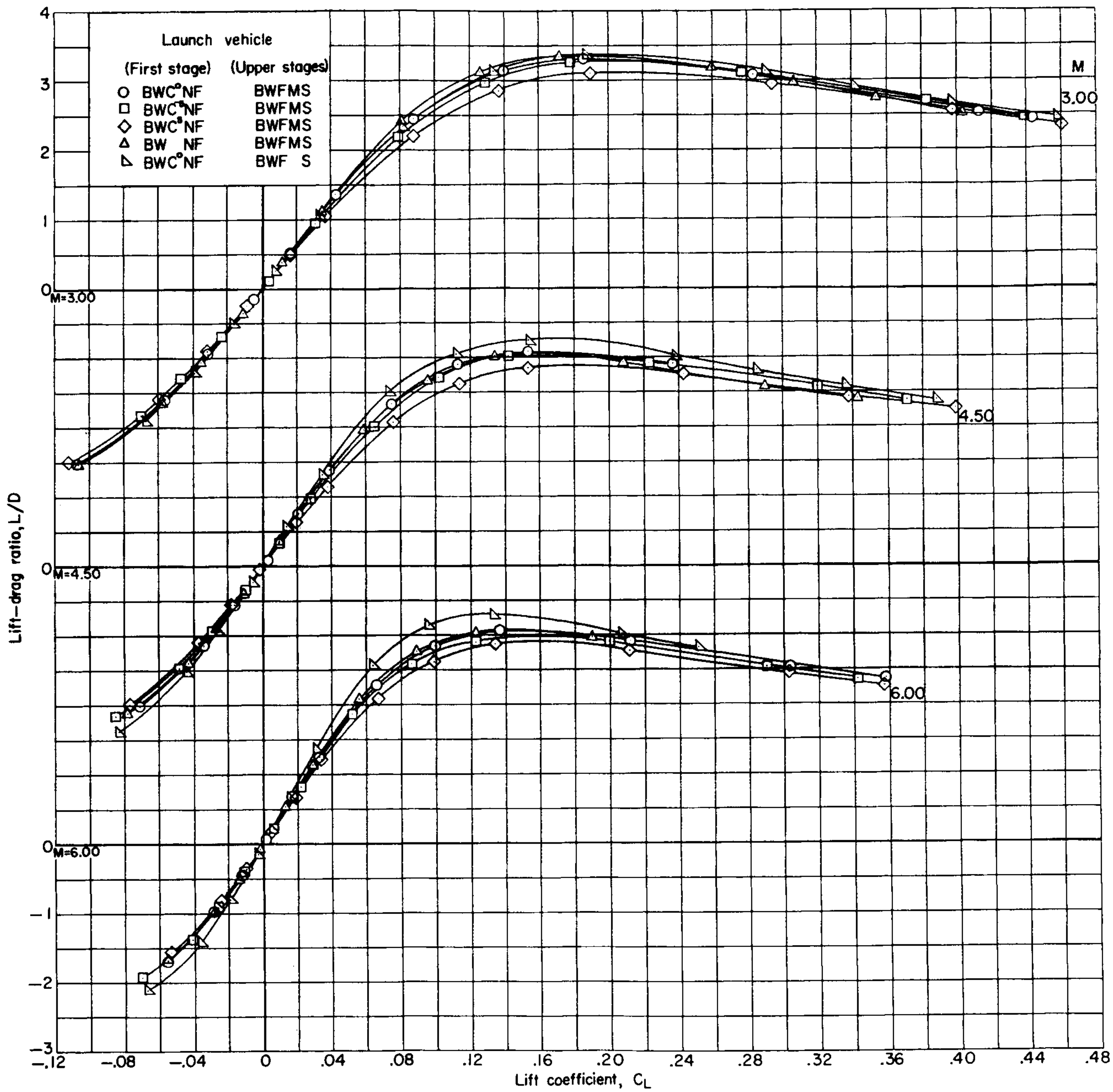

(d) Variation of lift-drag ratio with lift coefficient.

Figure 6.- Concluded.

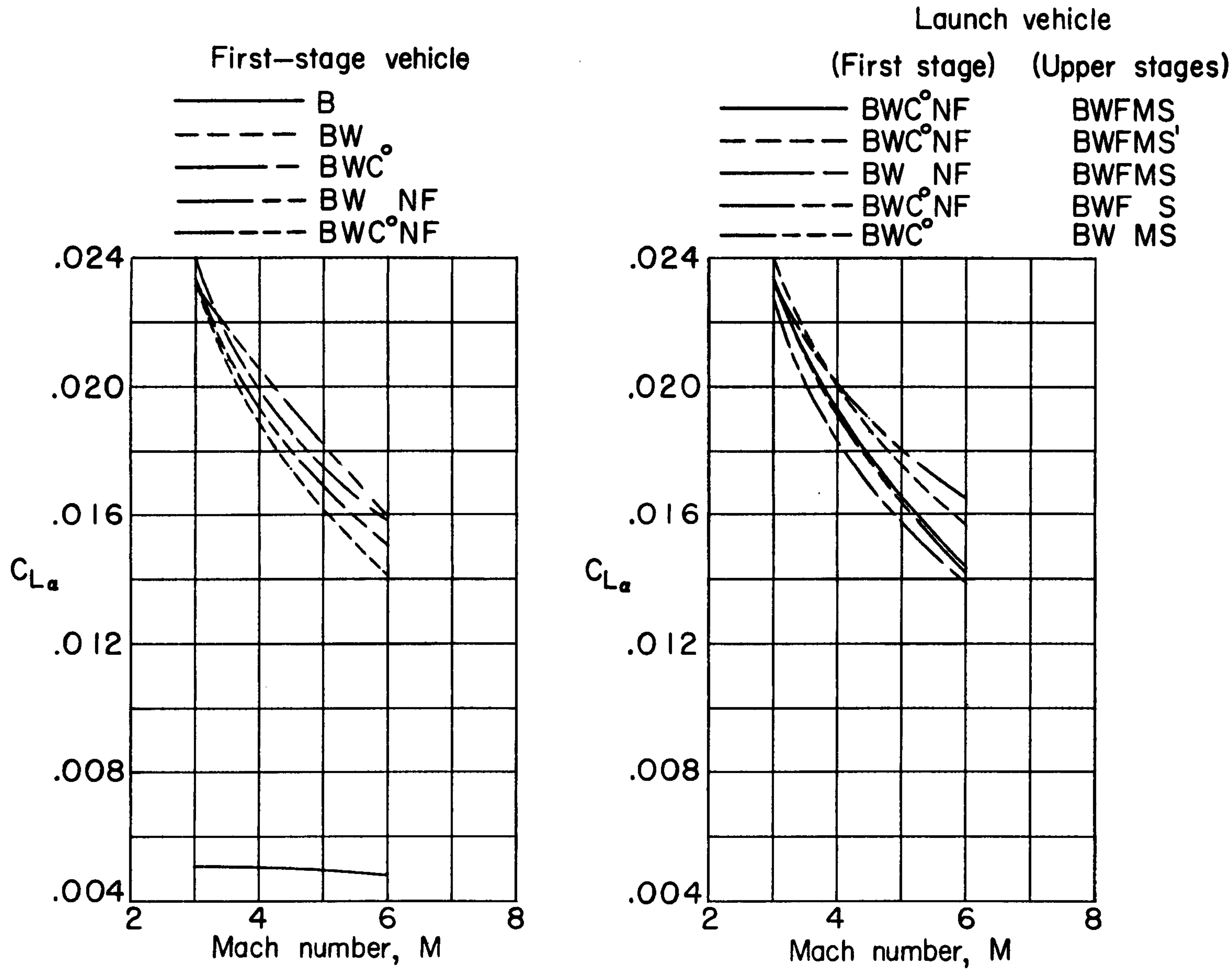

Figure 7.- Variation with Mach number of the lift-curve slopes for several modifications of the first stage and launch vehicle.

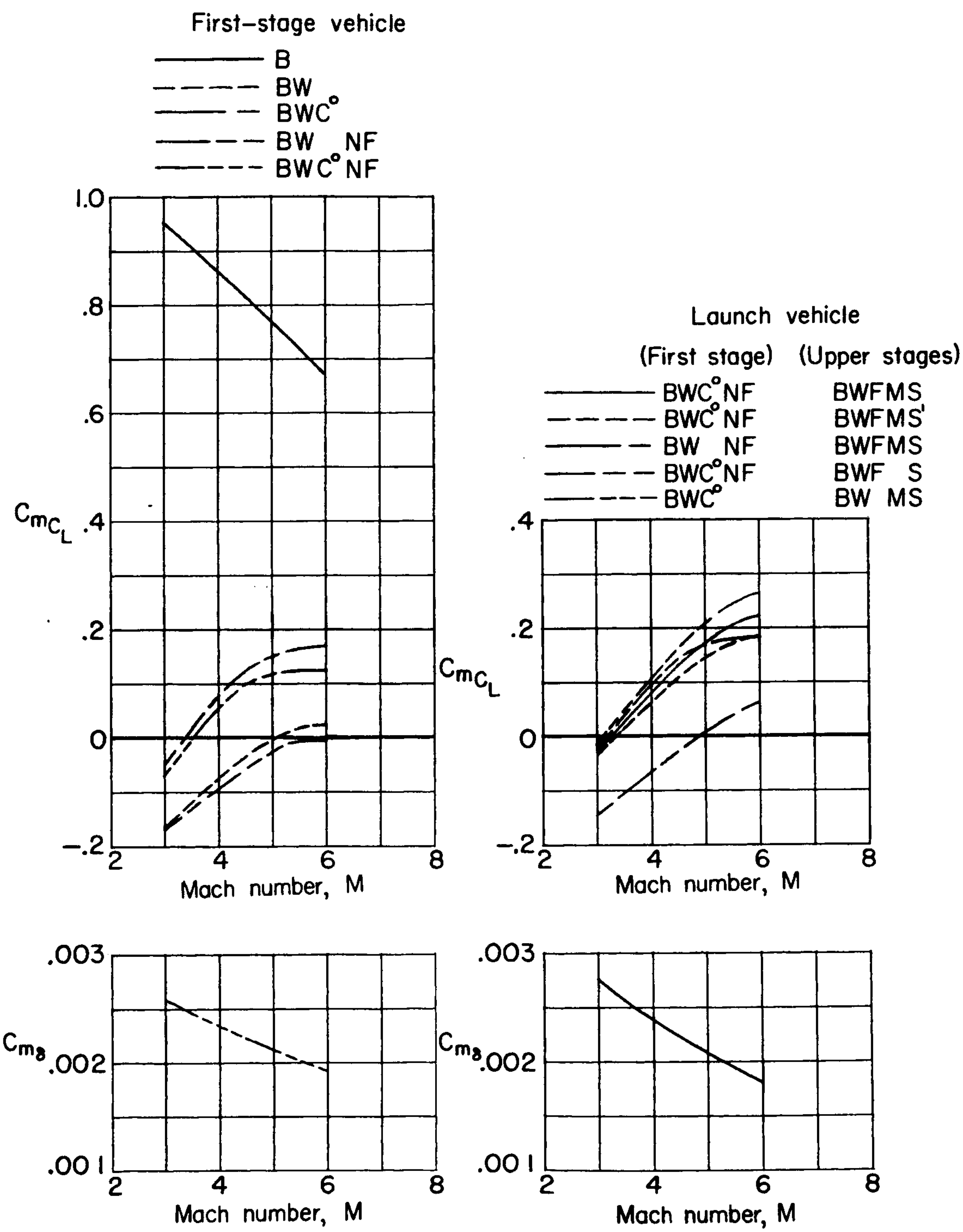

Figure 8.- Variation with Mach number of the longitudinal-stability parameter for several modifications of the first stage and launch vehicle and the canard effectiveness parameter for the complete first stage and complete launch vehicle.

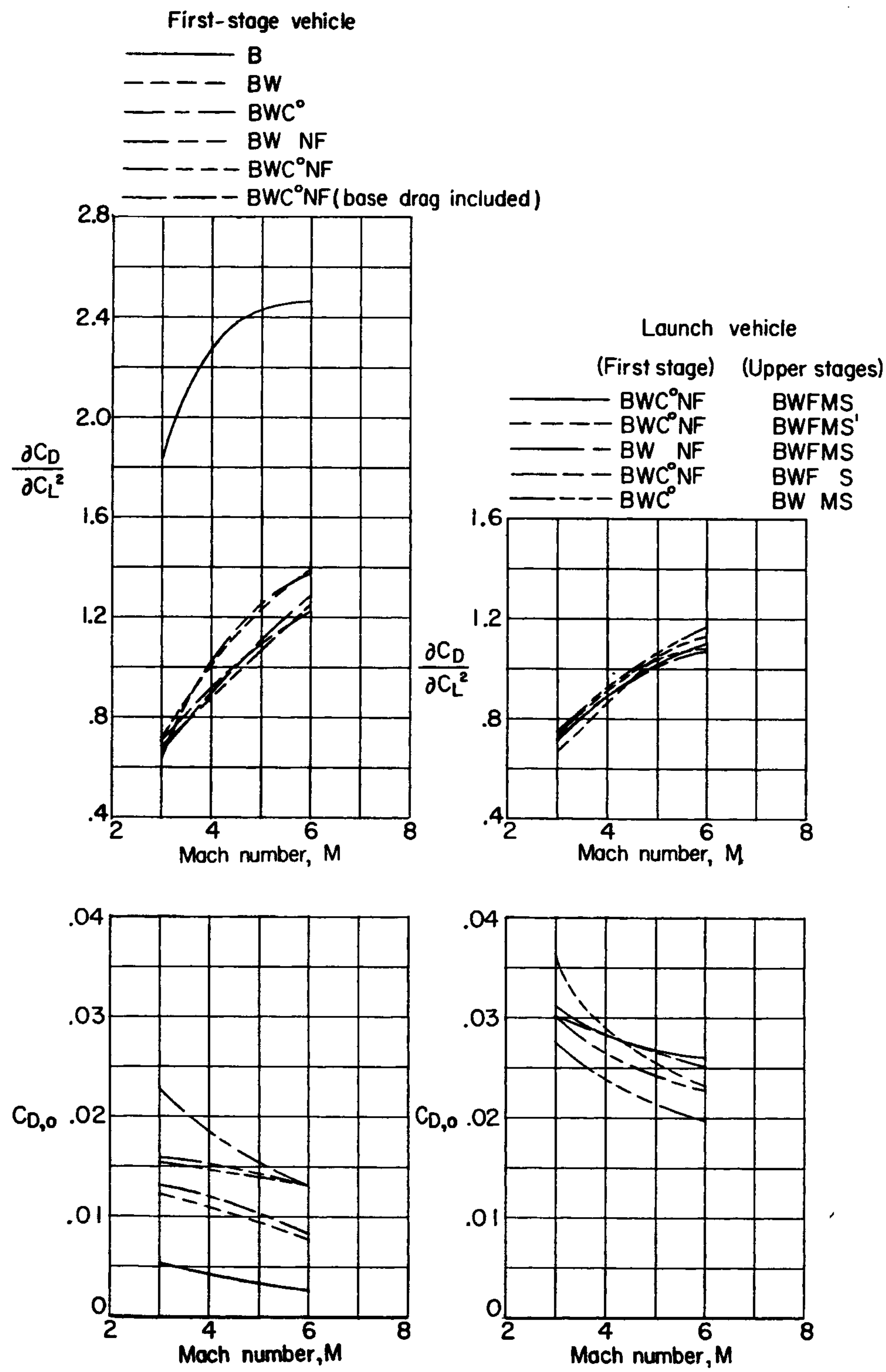

Figure 9.- Variation with Mach number of the drag at zero lift and the drag-due-to-lift parameter for several modifications of the first stage and launch vehicle.

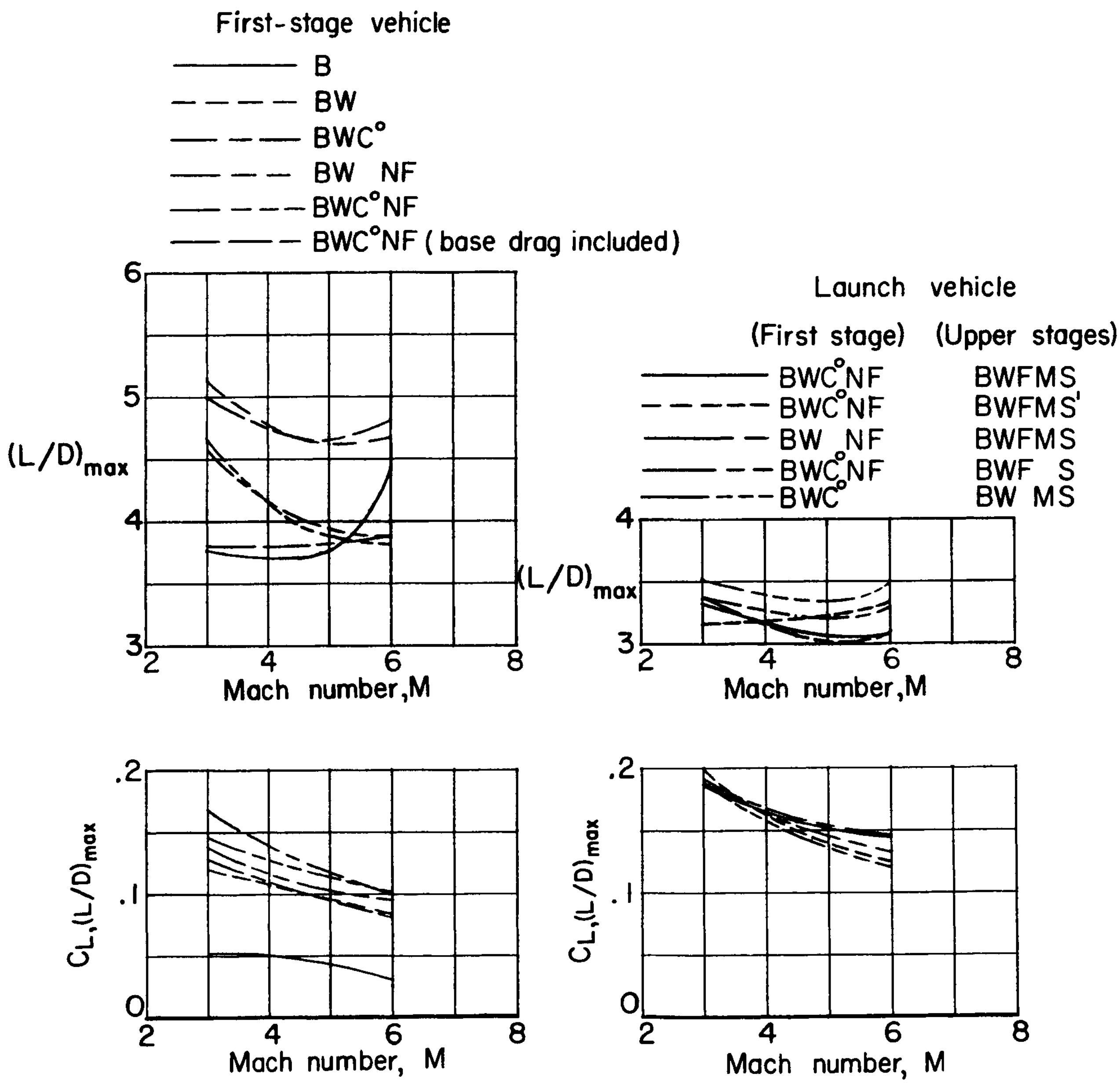

Figure 10.- Variation with Mach number of the maximum lift-drag ratio and the lift coefficient at which maximum lift drag occurs for several modifications of the first stage and launch vehicle.

NASA-Langley, 1964 L-4033